# General Disclaimer

## One or more of the Following Statements may affect this Document

- This document has been reproduced from the best copy furnished by the organizational source. It is being released in the interest of making available as much information as possible.

- This document may contain data, which exceeds the sheet parameters. It was furnished in this condition by the organizational source and is the best copy available.

- This document may contain tone-on-tone or color graphs, charts and/or pictures, which have been reproduced in black and white.

- This document is paginated as submitted by the original source.

- Portions of this document are not fully legible due to the historical nature of some of the material. However, it is the best reproduction available from the original submission.

PSU IRL-SCI-434

Classification Numbers 1.2, 1.6.2, 1.9.2, 3.2.2

# THE PENNSYLVANIA STATE UNIVERSITY

# IONOSPHERIC RESEARCH

## Scientific Report 434

# A FEASIBILITY STUDY OF A MICROWAVE WATER VAPOR MEASUREMENT FROM A SPACE PROBE ALONG AN OCCULTATION PATH

by

Richard L. Longbothum

April 15, 1975

## IONOSPHERE RESEARCH LABORATORY

## University Park, Pennsylvania

## DOCUMENT CONTROL DATA - R & D

*(Security classification of title, body of abstract and indexing annotation must be entered when the overall report is classified)*

| 1. ORIGINATING ACTIVITY (Corporate author) | 2a. REPORT SECURITY CLASSIFICATION |
|---|---|
| The Ionosphere Research Laboratory | 2b. GROUP |

**3. REPORT TITLE**

A Feasibility Study of a Microwave Water Vapor Measurement from a Space Probe Along an Occultation Path

**4. DESCRIPTIVE NOTES** *(Type of report and inclusive dates)*

Scientific Report

**5. AUTHOR(S)** *(First name, middle initial, last name)*

Richard L. Longbothum

| 6. REPORT DATE | 7a. TOTAL NO. OF PAGES | 7b. NO. OF REFS |
|---|---|---|
| April 15, 1975 | 64 | |

| 8a. CONTRACT OR GRANT NO. | 9a. ORIGINATOR'S REPORT NUMBER(S) |
|---|---|
| NASA NGL 39-009-003, NSF GA 33446 X 1 | |
| b. PROJECT NO. | PSU-IRL-SCI-434 |
| c. | 9b. OTHER REPORT NO(S) *(Any other numbers that may be assigned this report)* |
| d. | |

**10. DISTRIBUTION STATEMENT**

Supporting Agencies

| 11. SUPPLEMENTARY NOTES | 12. SPONSORING MILITARY ACTIVITY |
|---|---|
| | The National Aeronautics and Space Administration<br>The National Science Foundation |

**13. ABSTRACT**

The work presented is a preliminary feasibility study of stratospheric and mesospheric water vapor measurements using the microwave lines at 22 GHz (22.235 GHz) and 183 GHz (183.31 GHz).

The resonant cross sections for both the 22 GHz and the 183 GHz lines are presented and used to model the optical depth of atmospheric water vapor. The range of optical depths seen by a microwave radiometer through the earth's limb is determined from radiative transfer theory. Radiometer sensitivity, derived from signal theory, is compared with calculated optical depths to determine the maximum height to which water vapor can be measured using the following methods: passive emission, passive absorption, and active absorption.

The report concludes that measurements using the 22 GHz line are limited to about 50 km whereas the 183 GHz line will enable measurements up to and above 100 km for water vapor mixing ratios as low as 0.1 ppm under optimum conditions.

**DD** FORM 1 NOV 65 **1473** (PAGE 1)

Scientific Report 434

# A Feasibility Study of a Microwave Water Vapor
# Measurement from a Space Probe Along an Occultation Path

by

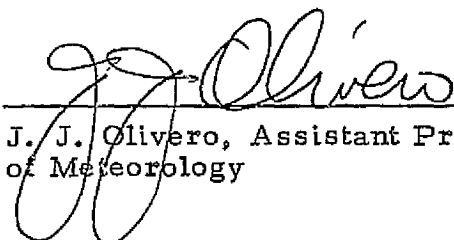Richard L. Longbothum

April 15, 1975

Submitted by:

J. J. Olivero, Assistant Professor
of Meteorology

Approved by:

J. S. Nisbet, Director
Ionosphere Research Laboratory

Ionosphere Research Laboratory

The Pennsylvania State University

University Park, Pennsylvania 16802

# ACKNOWLEDGEMENTS

# TABLE OF CONTENTS

# LIST OF FIGURES

# LIST OF TABLES

# TABLE OF SYMBOLS

A      is the amplitude of the signal

$|A(j\omega)|^2$ is the square of the overall transfer function of the RF amplifier, mixer, and IF amplifier

$B_{HF}$    is the noise bandwidth of the IF amplifier

$B_{LF}$    is the noise bandwidth of the low pass amplifier and integrator

C      is the resonant cross section scale height

$|H(j\omega)|^2$ is the square of the low pass filter and integrator transfer function

H'     is the differential optical depth scale height

$K_a(z)$   is the absorption coefficient in $cm^{-1}$

k      is Boltzmann's constant ($1.38 \times 10^{-23}$ Joules/$^{\circ}$K)

$n_o$      is the water vapor density at 30 km in molecules/$cm^3$

$\left.\begin{array}{c} n(z) \\ N(z) \end{array}\right\}$ is the water vapor density in molecules/$cm^3$

$n(t)$    is the input noise voltage

$\overline{P}_{D.C.}$ is the average power of the zero frequency component at the output of the square law detector

$R_s(\tau)$   is the autocorrelation function of the input signal

$R_n(\tau)$   is the autocorrelation function of the input noise

$R_{IF}(\tau)$   is the autocorrelation function at the output of the IF amplifier

$R_{Det}(\tau)$ is the autocorrelation function at the output of the square law detector

$R_{IF}^{signal}(\tau)$ is the autocorrelation function of the signal power at the output of the IF amplifier

$R_{IF}^{noise}(\tau)$ is the autocorrelation function of the noise power at the output of the IF amplifier

$R_{Det}^{s+n}(\tau)$ is the autocorrelation function of both signal and noise power at the output of the square law detector

$R_{Det}^{n \times n}(\tau)$ is the autocorrelation function of the noise power with itself at the output of the square law detector

$R_{Det}^{s \times n}(\tau)$ is the cross correlation function between the noise power and signal power at the output of the square law detector

$R_{Det}^{s \times s}(\tau)$ is the autocorrelation function of the signal power with itself at the output of the square law detector

$R_{out}^{s+n}(\tau)$ is the autocorrelation function of the total output signal and noise power

$s(t)$ is the input signal voltage

$T$ is the noise temperature at the receiver input from the following sources: the background noise from the sky, the atmospheric noise, the sidelobe noise, the noise from the losses of the antenna, etc.

$T$ is the kinetic temperature

$T_A$ is the unattenuated antenna temperature for any source, finite or extended in the antenna beam

$T_B$ is the excitation temperature of the gas (background temperature)

$T_R$ is the receiver noise temperature referred to the receiver input

$T_L$      is the noise from the antenna losses, sidelobe noise, etc.

$T_{SN} = T_A + T_R$ = total system noise temperature

$|T(\nu_o)|$  is the magnitude of the signal measured by a radiometer

$\overline{V^2_{Det}}$   is the mean square value of voltage developed across a one ohm resistor by $\overline{P}_{D.C.}$

$\overline{V}_{Det}$    is the average value of voltage developed across a one ohm resistor by $\overline{P}_{D.C.}$

$\overline{V}_e$      is the average value of voltage developed across a one ohm resistor that is due to the signal noise power

$V_o$      is the D.C. voltage that is injected into the low pass filter to cancel the noise component of the D.C. output

$\overline{V^2_{out}}$   is the mean square value of the output voltage

$\overline{V}_{out}$    is the D.C. value of the output voltage

$x(t)$     is the total voltage at the input of the receiver

$\alpha$       is the output signal to noise ratio

$\gamma$       is the randon phase angle

$\Delta P$      is the change in signal power

$\Delta T$      is the signal noise temperature

$\Delta T_{emission}$   is the signal due to emission

$\Delta T_{absorption}$   is the signal due to absorption

viii

$\Delta \nu$       is the total line width constant

$\Delta \nu_p$      is the line width constant of the pressure broadened line

$\Delta \nu_d$      is the line width constant of the Doppler broadened line

$\theta$        is the random phase of the signal

$\nu_o$        is the frequency of the signal

$\sigma_{absorption}(z)$ is the resonant cross section in $cm^2$

$\sigma_{scatter}(z)$ is the scattering cross section in $cm^2$

$\sigma_o$       is the resonant cross section at 30 km in $cm^2$

$\sigma_n^2$       is the average noise power at the output of the IF amplifier

$\sigma_s^2$       is the average signal power at the output of the IF amplifier

$\sigma_{out}^2$     is the variance of the output noise fluctuations

$\sigma_{out}^*$     is the relative deviation of the noise fluctuations from a D.C. signal level

$\tau (\nu, z, \phi)$ is the optical depth of the atmosphere which lies between the source and the radiometer

$\tau' (\nu, z, \phi)$ is the optical depth of the total atmosphere including any beyond the source

$\tau$        is the correlation function time delay

$\tau_I$       is the rise time of the integrator

$\Phi_{IN}(j\omega)$ is the power spectral density at the input to the receiver

$\Phi_{IF}(j\omega)$ is the power spectral density at the output of the IF amplifier

$\Phi_{Det}(j\omega)$ is the power spectral density at the output of the square law detector

$\Phi_{Det}^{D.C.}(j\omega)$ is the zero frequency term of the square law detector output spectral density

$\Phi_{IN}^{noise}(j\omega)$ is the spectral density of the input noise power

$\Phi_{IN}^{signal}(j\omega)$ is the spectral density of the input signal power

$\Phi_{IF}^{noise}(j\omega)$ is the spectral density of the noise power at the output of the IF amplifier

$\Phi_{IF}^{signal}(j\omega)$ is the spectral density of the signal power at the output of the IF amplifier

$\Phi_{Det}^{s+n}(j\omega)$ is the spectral density of the total power at the output of the square law detector

$\Phi_{Det}^{n \times n}(j\omega)$ is the spectral density of the noise-noise interaction noise power at the output of the square law detector

$\Phi_{Det}^{s \times n}(j\omega)$ is the spectral density of the noise-signal interaction noise power at the output of the square law detector

$\Phi_{Det}^{s \times s}(j\omega)$ is the spectral density of the signal-signal interaction signal power at the output of the square law detector

$\Phi_{out}^{s+n}(j\omega)$ is the spectral density of the total power at the receiver output

$\phi$     is the zenith angle in degrees

$\phi(\omega)$   is the phase factor of the RF amplifier, mixer and IF amplifier

$\omega_o$    is the frequency of the signal

# ABSTRACT

The work presented is a preliminary feasibility study of stratospheric and mesospheric water vapor measurements using the microwave lines at 22 GHz (22.235 GHz) and 183 GHz (183.31 GHz).

The resonant cross sections for both the 22 GHz and the 183 GHz lines are presented and used to model the optical depth of atmospheric water vapor. The range of optical depths seen by a microwave radiometer through the earth's limb is determined from radiative transfer theory. Radiometer sensitivity, derived from signal theory, is compared with calculated optical depths to determine the maximum height to which water vapor can be measured using the following methods: passive emission; passive absorption; and active absorption.

The report concludes that measurements using the 22 GHz line are limited to about 50 km whereas the 183 GHz line will enable measurements up to and above 100 km for water vapor mixing ratios as low as 0.1 ppm under optimum conditions.

# CHAPTER I

## INTRODUCTION

The question of how much water vapor exists in the stratosphere and above is one that has received attention for a considerable number of years but which has not yet been fully answered. The study of water vapor concentrations is important since water vapor and its dissociated products are active in the photochemistry of the stratosphere and mesosphere and thus effects ozone and contributes to the escape of hydrogen, for example. In addition it is thought to be responsible for hydrated ions, OH airglow emissions, and may control ionization loss processes as high as 80 km. Thus the amount of water vapor in the upper atmosphere is an important problem since it plays an important part in the chemistry and heat budget of the atmosphere.

On the basis of the above, it would appear that the measurement of water vapor concentrations in the upper atmosphere is of considerable importance to the scientific community. The best measurements of water vapor below 30 km were made with frost point hygrometers; however, these do not appear to be sensitive enough to the small concentrations of water vapor above about 30 km. They also suffer from the problem of local water vapor contamination.

The possibility of using radiometric methods for the detection and measurement of water vapor in the stratosphere and mesosphere was considered in a recent report (Longbothum, 1974). That report discusses the probable concentrations of water vapor and what is known about the microwave, millimeter wave, and infrared regions of the water vapor spectrum. The report concludes with a discussion of various methods of radiometric detection. The next logical step in

evaluation of a radiometric detection system is to examine the minimum

sensitivity of the various systems. This is the purpose of the present

report.

# CHAPTER II

## ABSORPTION CROSS SECTIONS

The microwave and millimeter wave regions will be examined in this report (Moody, (1971) reported that these were the only bands suitable for making measurements of water vapor concentration above 30 km). There are only two resonant water vapor lines in the microwave and millimeter wave regions: one at 22.235 GHz (1.35 cm); and the other located at 183.31 GHz (1.64 mm). The resonant cross sections are computed from relations A.1, A.2, A.3, A.4, and A.6 in appendix A using the relation

$$\sigma(h) = \frac{Ka(h)}{N(h)} \tag{1}$$

Table 1 is obtained for the centers of the resonant lines at 22.235 GHz amd 183.31 GHz. The above cross sections are plotted in Figure 1. The plot shows that the cross sections can be described (for the altitude range 30-80 km) by the function

$$\sigma(z) = \sigma_o e^{z/C} \tag{2}$$

where

$$C = \frac{\Delta z}{\Delta(\ln \sigma(z))} = 7.4 \text{ km}$$
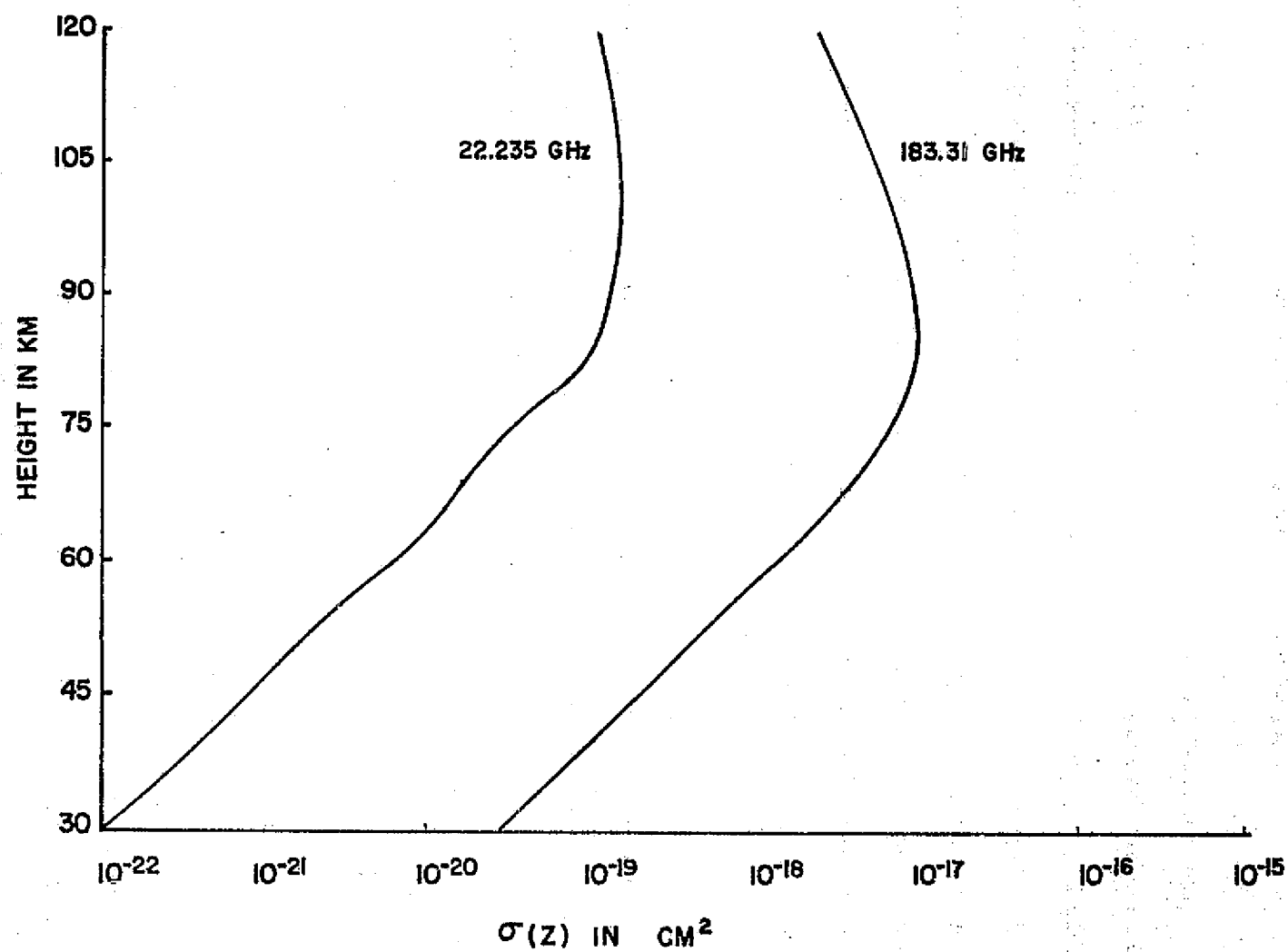
Figure 1  Absorption Cross Sections

Table 1: Absorption Cross Sections

| h | $\overset{*}{\Delta\nu}_{22}$ | $\overset{*}{\Delta\nu}_{183}$ | $\sigma_{22}$ (h) | $\sigma_{183}$ (h) |
|---|---|---|---|---|
| 30 km | $4.0 \times 10^7$ Hz | $4.0 \times 10^7$ Hz | $1.0 \times 10^{-22}$ cm$^2$ | $2.6 \times 10^{-20}$ cm$^2$ |
| 40 km | $9.7 \times 10^6$ Hz | $9.7 \times 10^6$ Hz | $4.0 \times 10^{-22}$ cm$^2$ | $9.5 \times 10^{-20}$ cm$^2$ |
| 50 km | $2.7 \times 10^6$ Hz | $2.7 \times 10^6$ Hz | $1.5 \times 10^{-21}$ cm$^2$ | $3.1 \times 10^{-19}$ cm$^2$ |
| 60 km | $6.6 \times 10^5$ Hz | $7.1 \times 10^5$ Hz | $6.1 \times 10^{-21}$ cm$^2$ | $1.3 \times 10^{-18}$ cm$^2$ |
| 70 km | $2.3 \times 10^5$ Hz | $3.3 \times 10^5$ Hz | $1.7 \times 10^{-20}$ cm$^2$ | $3.9 \times 10^{-18}$ cm$^2$ |
| 80 km | $5.0 \times 10^4$ Hz | $2.1 \times 10^5$ Hz | $6.6 \times 10^{-20}$ cm$^2$ | $8.3 \times 10^{-18}$ cm$^2$ |
| 90 km | $2.6 \times 10^4$ Hz | $2.1 \times 10^5$ Hz | $1.3 \times 10^{-19}$ cm$^2$ | $7.8 \times 10^{-18}$ cm$^2$ |
| 100 km | $2.8 \times 10^4$ Hz | $2.2 \times 10^5$ Hz | $1.4 \times 10^{-19}$ cm$^2$ | $5.8 \times 10^{-18}$ cm$^2$ |
| 110 km | $3.0 \times 10^4$ Hz | $2.5 \times 10^5$ Hz | $1.3 \times 10^{-19}$ cm$^2$ | $3.7 \times 10^{-18}$ cm$^2$ |
| 120 km | $3.5 \times 10^4$ Hz | $2.9 \times 10^5$ Hz | $1.0 \times 10^{-19}$ cm$^2$ | $1.9 \times 10^{-18}$ cm$^2$ |

5

* (See Appendix A)

# CHAPTER III

## OPTICAL DEPTH OF WATER VAPOR ABOVE 30 KM

The transmission of a plane atmosphere is described by the optical depth $\tau$ $(\nu, h, \phi)$ defined as

$$\tau(\nu, h, \phi) = \sum_i \int_h^\infty \sigma^i(z, \nu) n^i(z) \sec \phi \, dz \qquad (3)$$

where

$\sigma^i(z, \nu) = \sigma^i_{scatter}(z, \nu) + \sigma^i_{absorption}(z, \nu)$

         = the total extinction cross section, in $cm^2$, for the ith

         constituent

$n^i(z)$     = the number density of the ith constituent in molecules $\cdot$ $cm^{-3}$

$\phi$       = the zenith angle in degrees

Spherical atmospheres can be treated with this expression for zenith angles less than about $80^\circ$. However, for zenith angles greater than $80^\circ$, the Chapman Function must be used in place of $\sec \phi$ (Rishbeth, et al., 1969). For the sake of simplicity, the plane atmosphere solution will be used for this report.

For the molecules, atoms, and particles above 30 km, non-resonant scattering can be neglected in general. Thus only the resonant absorption cross section will be retained in the expression for optical depth. Also in the frequency spectrum near the two water vapor lines, only four other molecules have resonant absorption (emission) lines (Longbothum, 1974). They are $O_3$, $SO_2$, $NO_2$, and $N_2O$. The concentrations of $SO_2$, $NO_2$ and $N_2O$ are thought to be very small. The concentration of $O_3$ above 30 km, follows quite closely that of $H_2O$ and must be considered in the case of the 183.31 GHz water vapor line. This possible complication will be dealt with in a

future study. For the present only water vapor will be considered.

It was suggested in the recent report (Longbothum, 1974) that the most probable water vapor concentrations lie between 0.1 ppm and 10.0 ppm. Thus a value of $n_{min}$ corresponding to 0.1 ppm and a value of $n_{max}$ corresponding to 10 ppm will be used to calculate $\tau_{min}$ and $\tau_{max}$ respectively.

The product $\sigma(z) n(z)$, the differential optical depth, is plotted in Figure 2. This shows that for the height range up to about 80 km, the product $\sigma(z) n(z)$ is relatively constant and approximately equal to $\sigma_o n_o$. Above 80 km, the product is height dependent and can be described by the function

$$\sigma(z) n(z) = \sigma_o n_o \exp \left[ - (z - 80 \text{ km})/ H' \right] \qquad (4)$$

where $\qquad H' = \dfrac{-\Delta z}{\Delta \ln \left[ n(z) \cdot \sigma(z) \right]} = 6 \text{ km}$

$\qquad\qquad$ for the 22.235 GHz line

and

$\qquad H' = 5 \text{ km}$ for the 183.31 GHz line.

The vertical optical depth ($\phi = 0$) can be integrated for the two ranges of z to yield

$$= \begin{cases} n_o \sigma_o \left[ (80 \text{ km} - h) + H' \right] & h < 80 \text{ km} \qquad (5) \\ n_o \sigma_o \, H' \exp \left[ -(h - 80 \text{ km})/H' \right] & h > 80 \text{ km} \end{cases}$$

The average value of $n_o \sigma_o$ is $3.4 \times 10^{-10} \text{cm}^{-1}$ for the 22.235 GHz line and $8.0 \times 10^{-8} \text{cm}^{-1}$ for the 183.31 GHz line. These values are based on Figure 2. Table 2, also obtained using these values, shows that attenuation will be slight at 22.235 GHz and quite significant at 183.31 GHz.
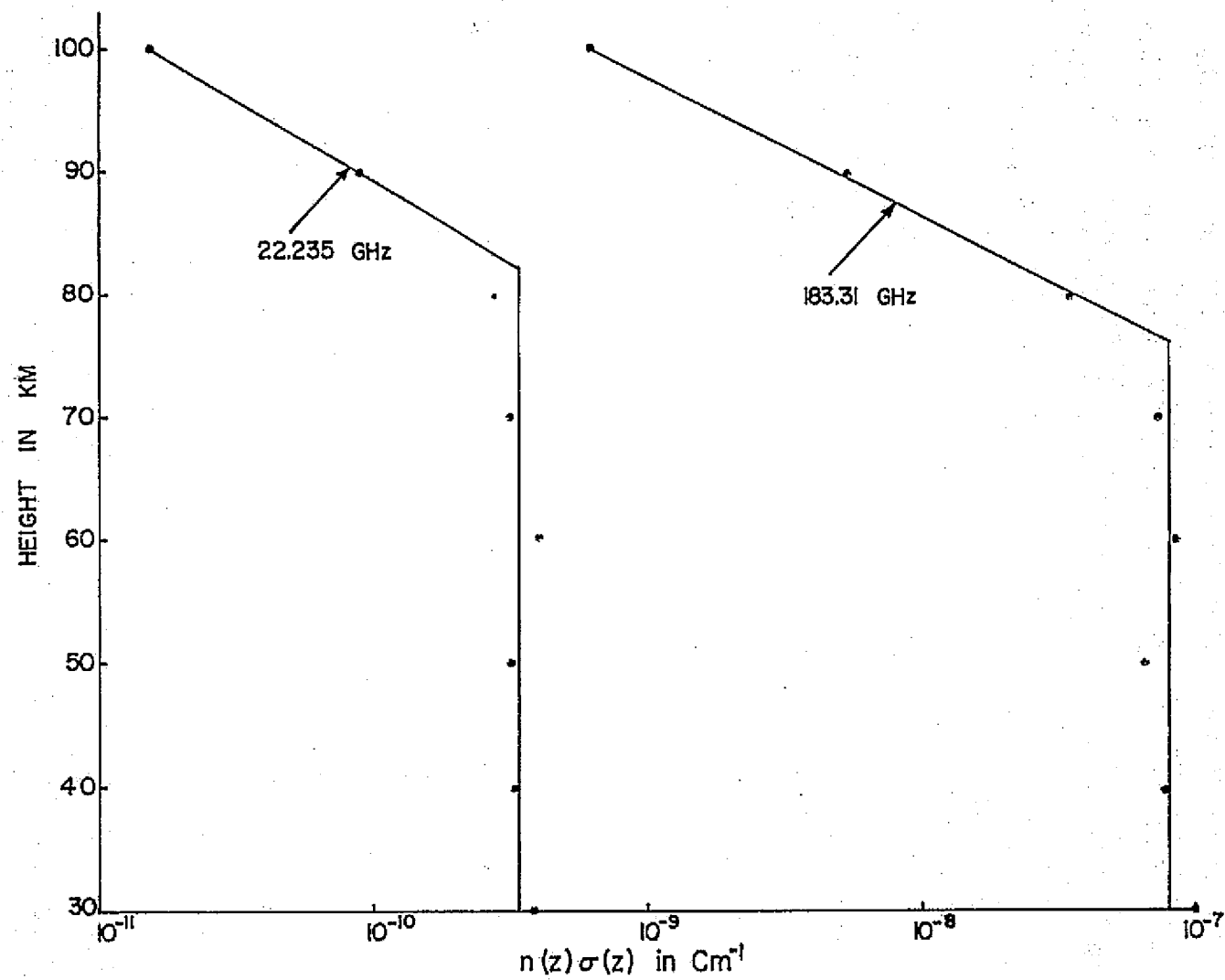
Figure 2  Differential Optical Depths

8

Table 2: Atmospheric Zenith Optical Depths Due to Water Vapor

| | 22.235 GHz | | 183.31 GHz | |
| | $\tau_{min}$ (0.1 ppm) | $\tau_{max}$ (10 ppm) | $\tau_{min}$ (0.1 ppm) | $\tau_{max}$ (10 ppm) |
| h | | | | |
|---|---|---|---|---|
| 30 km | $1.87 \times 10^{-5}$ | $1.87 \times 10^{-3}$ | $4.38 \times 10^{-3}$ | $4.38 \times 10^{-1}$ |
| 40 km | $1.54 \times 10^{-5}$ | $1.54 \times 10^{-3}$ | $3.59 \times 10^{-3}$ | $3.59 \times 10^{-1}$ |
| 50 km | $1.20 \times 10^{-5}$ | $1.20 \times 10^{-3}$ | $2.79 \times 10^{-3}$ | $2.79 \times 10^{-1}$ |
| 60 km | $8.70 \times 10^{-6}$ | $8.70 \times 10^{-4}$ | $1.99 \times 10^{-3}$ | $1.99 \times 10^{-1}$ |
| 70 km | $5.35 \times 10^{-6}$ | $5.35 \times 10^{-4}$ | $1.20 \times 10^{-3}$ | $1.20 \times 10^{-1}$ |
| 80 km | $2.01 \times 10^{-6}$ | $2.01 \times 10^{-4}$ | $3.98 \times 10^{-4}$ | $3.98 \times 10^{-2}$ |
| 90 km | $3.79 \times 10^{-7}$ | $3.79 \times 10^{-5}$ | $5.39 \times 10^{-5}$ | $5.39 \times 10^{-3}$ |
| 100 km | $7.16 \times 10^{-8}$ | $7.16 \times 10^{-6}$ | $7.30 \times 10^{-6}$ | $7.30 \times 10^{-4}$ |
| 110 km | $1.35 \times 10^{-8}$ | $1.35 \times 10^{-6}$ | $9.88 \times 10^{-7}$ | $9.88 \times 10^{-5}$ |
| 120 km | $2.56 \times 10^{-9}$ | $2.56 \times 10^{-7}$ | $1.34 \times 10^{-7}$ | $1.34 \times 10^{-5}$ |

# CHAPTER IV

# RADIATIVE TRANSFER

To measure water vapor concentrations using a radiometer, one must establish the relationship between various sources of radiation, the atmospheric optical depth $\tau$, and the radiation that the receiving antenna intercepts. This relation is given by the theory of radiative transfer.

Consider an antenna connected to a receiver. The antenna is viewing a source (temperature $T_A$) at a great distance through the relatively cold atmosphere (temperature $T_B$) that lies between the two. This atmosphere has an optical depth $\tau(\nu_o)$. If one includes the atmosphere which lies beyond the source also, then the total optical depth is $\tau'(\nu_o)$. The temperature that the antenna will see then is given by the solution of the equation of radiative transfer (Barrett, 1964).

$$T(\nu_o) = T_A e^{-\tau(\nu_o)} + T_B \left[1 - e^{-\tau'(\nu_o)}\right] \tag{6}$$

where

$T(\nu_o)$ is the received antenna temperature for frequency $\nu_o$

$T_A$ is the unattenuated temperature for any source, finite or extended in the antenna beam.

$T_B$ is the excitation temperature of the gas (background temperature).

$\tau(\nu_o)$ is the optical depth of the gas between the observer and the source

and

$\tau'(\nu_o)$ is the optical depth of the total gas including any beyond the source.

When the radiometer is tuned to $\nu$ (not a resonant frequency of the atmospheric gas), the optical depths change to new values $\tau(\nu)$ and

$\tau'(\nu)$ and the change in antenna temperature between $T(\nu_o)$ and $T(\nu)$ is

$$\Delta T = T(\nu_o) - T(\nu) = T_A \left[ e^{-\tau(\nu_o)} - e^{-\tau(\nu)} \right]$$

$$+ T_B \left[ e^{-\tau'(\nu)} - e^{-\tau'(\nu_o)} \right] \tag{7}$$

$\Delta T$ represents the difference signal measured by a receiver as it is tuned through the resonant line at $\nu_o$. However, $\Delta T$ will include both absorption and emission effects of the gas. In order to make a more accurate measurement, there must be some method of separating the two responses. If the antenna is directed away from the source or (in case of an active experiment) the transmitter is turned off, then $\Delta T$ is the signal from the emissions of the gas.

$$\Delta T_{emission} = \Delta T'(\nu_o, \nu) = T_B \left[ e^{-\tau'(\nu)} - e^{-\tau'(\nu_o)} \right]$$

$$\cong T_B \tau'(\nu_o) \quad \text{for} \quad 1 >> \tau'(\nu_o) >> \tau'(\nu) \tag{8}$$

This approximation is generally valid since the values $\tau'(\nu)$ and $\tau(\nu)$ are due to all the nonresonant extinction processes such as wings of higher order lines and scattering. Thus they are much smaller than the resonant optical depths $\tau'(\nu_o)$ and $\tau(\nu_o)$.

If $\Delta T'$ is subtracted from $\Delta T$, the contribution due to absorption only is obtained.

$$\Delta T_{absorption} = \Delta T''(\nu_o, \nu) = T_A \left[ e^{-\tau(\nu_o)} - e^{-\tau(\nu)} \right]$$

$$\cong -T_A \tau(\nu_o) \quad \text{for} \quad 1 >> \tau(\nu_o) >> \tau(\nu) \tag{9}$$

The measurement only involves the magnitude of the signal thus the relations between the receiver input and the atmosphere are

$$|\Delta T' (\nu_o)| \cong T_B \tau' (\nu_o) \tag{10}$$

for an emission experiment and

$$|\Delta T'' (\nu_o)| \cong T_A \tau (\nu_o) \tag{11}$$

for an absorption experiment.

For most conceivable experiments

$$\tau (\nu_o) \cong \tau' (\nu_o)$$

so that a common expression can be written for both measurements

$$|\Delta T (\nu_o)| \cong T_S \tau (\nu_o) \tag{12}$$

where $T_S$ is the source temperature and is given by

$$T_S = \begin{cases} T_A & \text{for absorption} \\ T_B & \text{for emission} \end{cases}$$

This is the equation that couples the atmosphere to the radiometer. However, in order to detect a water vapor concentration, one must have

$$|\Delta T (\nu_o)| \geq \Delta T_{min} \tag{13}$$

or equivalently

$$|\Delta P (\nu_o)| \cong P_S \tau (\nu_o) \geq \Delta P_{min}$$

where $\Delta T_{min}$ is the minimum detectable temperature the radiometer can sense and is limited by the noise in both source and receiver; $\Delta P_{min}$ is the minimum detectable change in signal power that can be sensed by the radiometer and $P_S$ is the radiated power of the source.

# CHAPTER V

## RADIOMETER SENSITIVITY

The expression for $\Delta T_{min}$ (see appendixes B and C) is

$$\Delta T_{min} \cong \frac{2 T_{SN} \alpha}{\sqrt{Bt}}$$

(B. 24)

for a voltage signal to noise ratio $\alpha$ and where

$$T_{SN} = T_R + T_S + T_L \qquad \text{for a thermal source and}$$

$$T_{SN} = T_R + T_L \qquad \text{for a nonthermal source.}$$

$T_R$ = the noise temperature of the receiver

$T_L$ = the noise from antenna losses, sidelobe noise, etc.

$B$ = the receiver bandwidth in $H_z$

and t is the post detection integration time in seconds of the receiver.

Notice that if $T_S \gg T_R + T_L$ then there is nothing to be gained by

building a better receiver since the noise fluctuations will be due to the

source. Thus the limiting factor on absorption measurements will be

the source noise in the case of a thermal source.

A minimum measurement can be made only if the equality holds

in equation (13). This measurement can be enhanced by slant path

viewing, thus the relationship becomes

$$\frac{\tau(\nu_o)}{\sec \phi} = \frac{\tau_{min}}{\sec \phi} = \frac{\Delta T_{min}}{T_S \sec \phi} =$$

$$\frac{2}{\sqrt{Bt}} \quad \frac{\alpha}{\sec \phi} \quad \left( 1 + \frac{T_R + T_L}{T_S} \right)$$

(14)

It would appear that one could reduce $\tau$ by increasing B or t in the above equation. However, t is limited by the amount of available observing time and desired spatial resolution. This is determined by a change in source position as a function of time, by a time dependent change in the power received by the antenna, or by the time of flight of the vehicle. Also, t can not be increased beyond the point where it begins to distort the true source profile (Kraus, 1966). For rockets, the time of flight would limit the integration time to $10^0$ - $10^1$ seconds. For a satellite, the time range would be about $10^1$ - $10^2$ seconds. For a balloon, the time range would be about $10^1$ - $10^3$ seconds.

The bandwidth B can not be made too wide or there will be a loss of spectral information and interference from radio signals of terrestrial origin (Kraus, 1966). Also B will be limited by the bandwidth of the signal, the current state of equipment development, and many other factors. B has a maximum value of about $10^{10}$ Hz, but is only about 200 MHz for low noise receivers (Staelin, 1969).

System noise temperatures of radiometers have for years been the limiting factor in sensitivity. Values of system temperature have been about $3000^oK$ for 22.235 GHz radiometers to about $70,000^oK$ for 183.31 GHz radiometers. (See Figure 3). This figure shows the state of the art system noise temperatures that existed 5 to 10 years ago. However, there has been a major breakthrough in mixer development in the last few years. Current values for system noise temperatures range from about $600^oK$ for 1.3 cm radiometers to about $4000^oK$ for 2 mm radiometers (Buhl et al., 1971). Staelin (1973) also reports that system noise temperatures less than $300^oK$ at frequencies up to 200 GHz may be possible with cooled Schottky barrier diodes. Waters (1974)
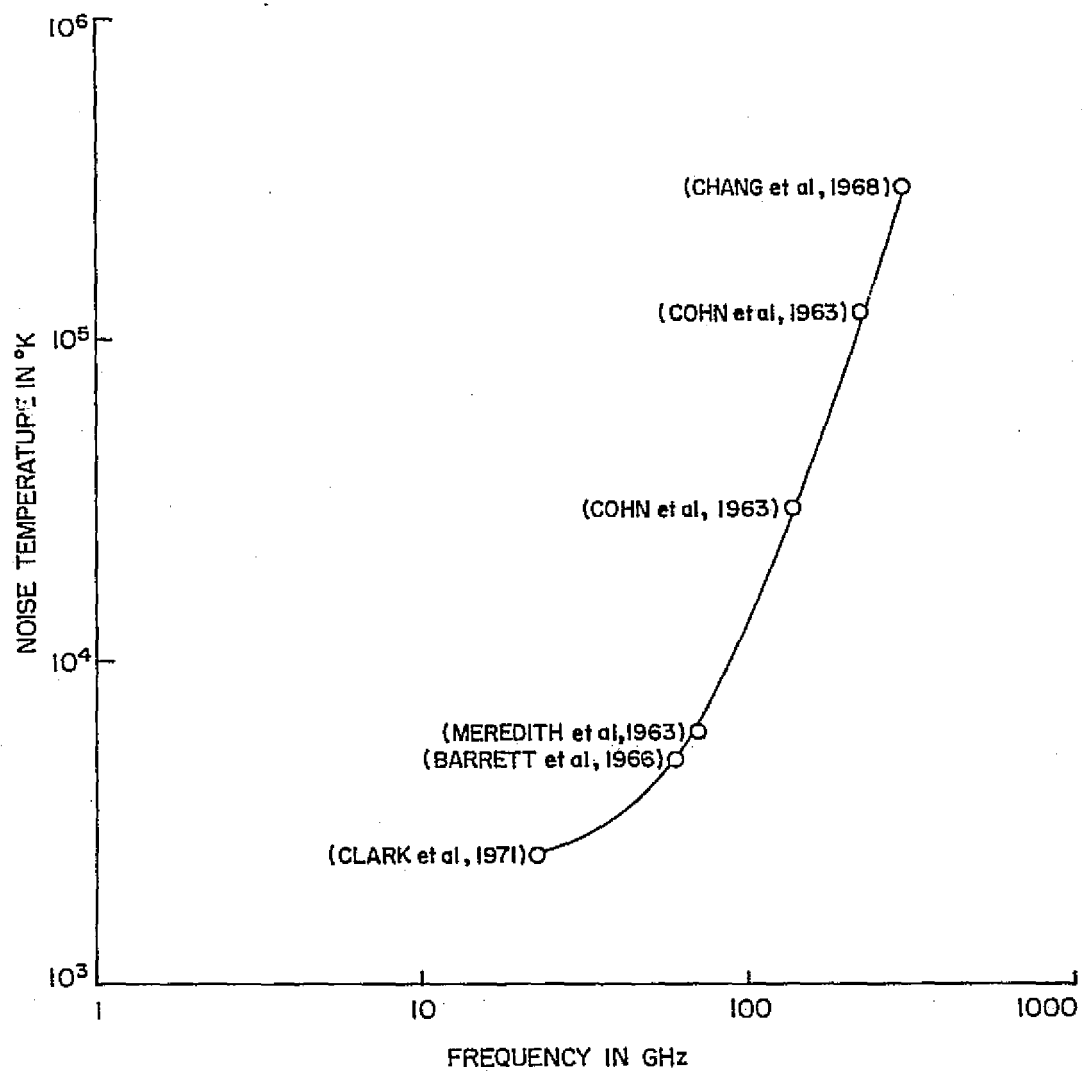
Figure 3  Noise Temperatures of Receivers

gives a state of the art system temperature of $1200^{\circ}$K at 183 GHz. Thus for this report the value of $T_R + T_L$ will be taken as $600^{\circ}$K for the 22.235 GHz line and $1200^{\circ}$K for the 183.31 GHz line.

The apparent source temperature, $T_S$, must be specified for each possible experiment. For atmospheric emission $T_S$ is assumed to be $300^{\circ}$K. For an absorption experiment using the solar disc as an external source, $T_S \cong 10,000^{\circ}$K for the 22.235 GHz region and $T_S \cong 6,000^{\circ}$K for the 183.31 GHz region of the solar spectrum (Linsky, 1973). An active experiment using a 10 milliwatt broadband source (for a receiving antenna effective area $A_e = 10$ M$^2$, a transmitter antenna gain of 100, and a distance of $3 \times 10^6$ meters between the receiver and transmitter) has a value of $P_S$

$$P_S = \frac{P_T \ GA_e}{4 \pi R^2} = 8.84 \times 10^{-14} \text{ Watts} \tag{15}$$

# CHAPTER VI

## COMPARISONS OF EXPERIMENTAL CONFIGURATIONS

There are three basic experiments that can be performed now. An emission experiment, a passive absorption experiment, and an active absorption experiment. These can be performed at 22.235 GHz or at 183.31 GHz. The experiment at 22.235 GHz suffers from weak line strength, but has the advantage of greater receiver sensitivity and less interference from other lines. The experiment at 183.31 GHz has a resonant cross section on the order of 200 times greater, but suffers from less sensitive detectors, and more interference from higher order lines so that equipment having very good resolution will be required. Both lines will be considered below, six figures are presented corresponding to the six possibilities to follow, B will be taken to be $\Delta \nu$ of the line and sec $\phi$ will be taken equal to 10. This will correspond to an occultation experiment (Longbothum, 1974).

### 6.1 Passive Resonant Emission

This experiment has the advantage that it does not require a source and can be performed at any time. The method is, however, an order of magnitude less sensitive to water vapor concentrations (Longbothum, 1974).

The minimum optical depth that can be detected is given by

$$\tau_{min} = \frac{\Delta T_{min}}{T_S \sec \phi} = \frac{2 \alpha}{\sqrt{t \Delta \nu}} \left( \frac{1}{10} + \frac{60}{T_S} \right) \tag{16}$$

for the 22.235 GHz line, and

$$\tau_{min} = \frac{\Delta T_{min}}{T_S \sec \phi} = \frac{2\alpha}{\sqrt{t}\, \Delta\nu} \left( \frac{1}{10} + \frac{120}{T_S} \right)$$

(17)

for the 183.31 GHz line.

The values of $T_S$ in these expressions is taken as the average of the temperatures at height h and at 5 km above h. The values of $T_S$ obtained are (U.S. Standard Atmosphere, 1962).

| h | $T_S$ | h | $T_S$ |
|---|---|---|---|
| 30 km | 237°K | 80 km | 181°K |
| 40 km | 257°K | 90 km | 188°K |
| 50 km | 269°K | 100 km | 224°K |
| 60 km | 248°K | 110 km | 286°K |
| 70 km | 210°K | 120 km | 411°K |

The maximum signal to noise ratio $\alpha$ is taken as 10 and the minimum is taken as 1. The maximum time t is taken as 100 sec and the minimum time is taken as 1 sec. Thus the ratio $\alpha/\sqrt{t}$ will range from 10 to 0.1.

Table 3 of minimum detectable optical depths is obtained from equations 16 and 17. These values reflect the increased ratiometer sensitivity at lower frequencies (see figure 3).

Based on the limiting value of atmospheric optical depth presented in Table 2 and the minimum detectable optical depths presented in Table 3, Figures 4 and 5 are obtained. These figures show that at 22.235 GHz, water vapor can be measured to about 70 km under optimum conditions. However, the more realistic limit would be about 50 km. When the experiment is performed at 183.31 GHz,

Table 3: Minimum Detectable Optical Depths for Passive Emission ($\Delta T_{min}/T_S$ sec $\phi$)

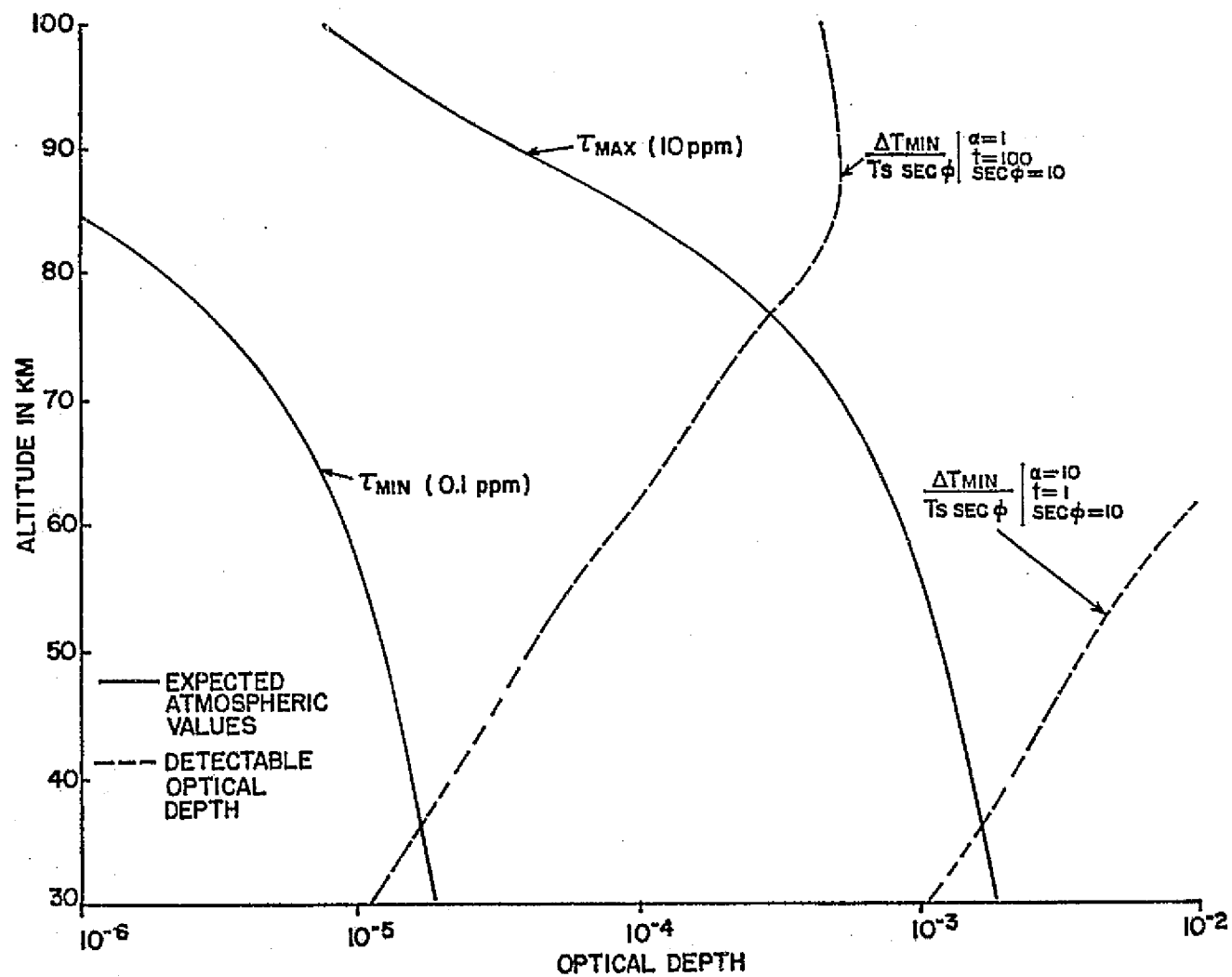| h | 22.235 GHz | | 183.31 GHz | |
|---|---|---|---|---|
| | $\dfrac{\alpha}{\sqrt{t}} = 0.1$ | $\dfrac{\alpha}{\sqrt{t}} = 10$ | $\dfrac{\alpha}{\sqrt{t}} = 0.1$ | $\dfrac{\alpha}{\sqrt{t}} = 10$ |
| 30 km | $1.1 \times 10^{-5}$ | $1.1 \times 10^{-3}$ | $1.9 \times 10^{-5}$ | $1.9 \times 10^{-3}$ |
| 40 km | $2.1 \times 10^{-5}$ | $2.1 \times 10^{-3}$ | $3.6 \times 10^{-5}$ | $3.6 \times 10^{-3}$ |
| 50 km | $3.9 \times 10^{-5}$ | $3.9 \times 10^{-3}$ | $6.7 \times 10^{-5}$ | $6.7 \times 10^{-3}$ |
| 60 km | $8.4 \times 10^{-5}$ | $8.4 \times 10^{-3}$ | $1.4 \times 10^{-4}$ | $1.4 \times 10^{-2}$ |
| 70 km | $1.6 \times 10^{-4}$ | $1.6 \times 10^{-2}$ | $2.3 \times 10^{-4}$ | $2.3 \times 10^{-2}$ |
| 80 km | $3.9 \times 10^{-4}$ | $3.9 \times 10^{-2}$ | $3.3 \times 10^{-4}$ | $3.3 \times 10^{-2}$ |
| 90 km | $5.2 \times 10^{-4}$ | $5.2 \times 10^{-2}$ | $3.2 \times 10^{-4}$ | $3.2 \times 10^{-2}$ |
| 100 km | $4.4 \times 10^{-4}$ | $4.4 \times 10^{-2}$ | $2.7 \times 10^{-4}$ | $2.7 \times 10^{-2}$ |
| 110 km | $3.6 \times 10^{-4}$ | $3.6 \times 10^{-2}$ | $2.1 \times 10^{-4}$ | $2.1 \times 10^{-2}$ |
| 120 km | $2.6 \times 10^{-4}$ | $2.6 \times 10^{-2}$ | $1.5 \times 10^{-4}$ | $1.5 \times 10^{-2}$ |

Figure 4  22.235 GHz Emission Experiment
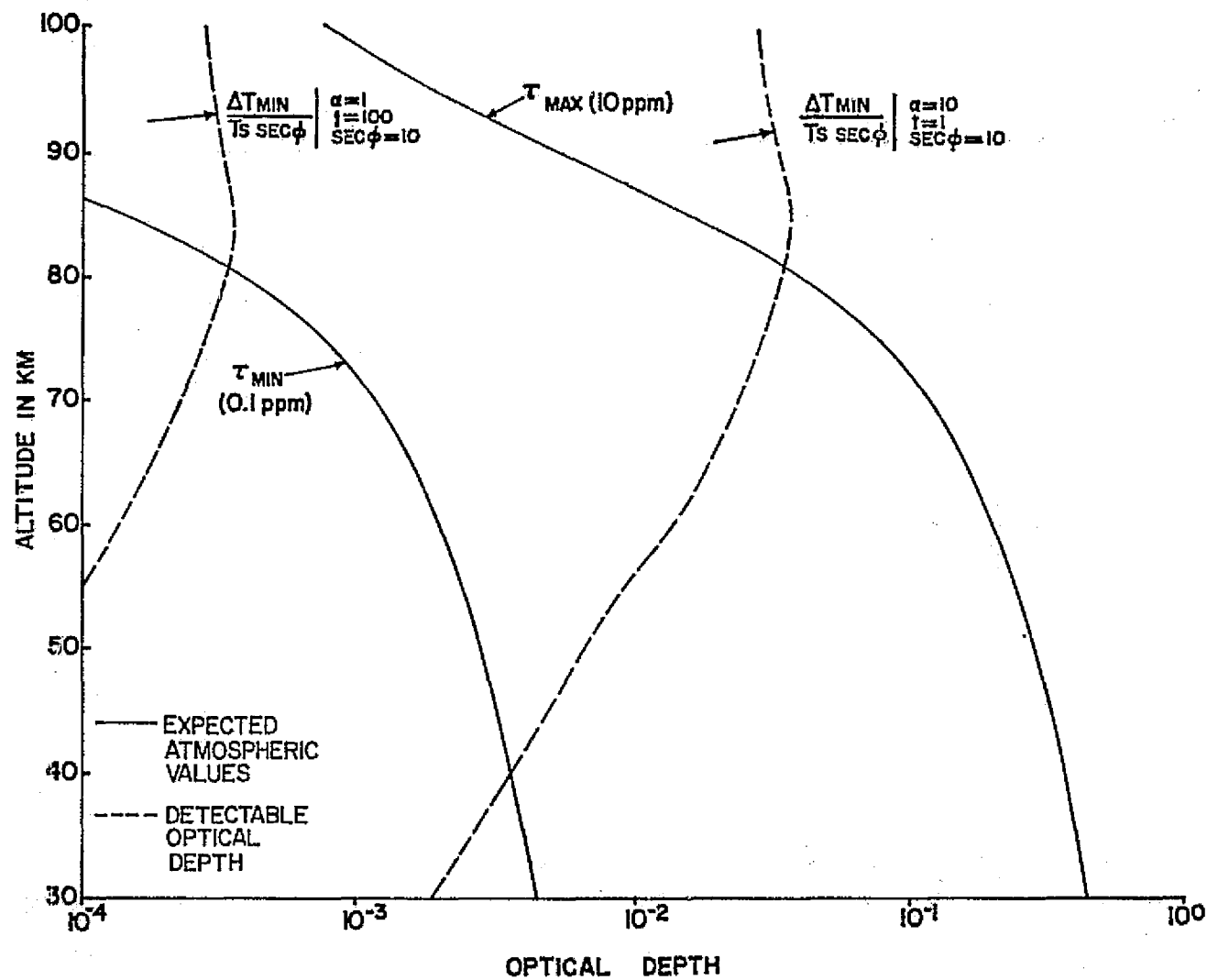
Figure 5  183.31 GHz Emission Experiment

the situation is improved. For optimum conditions, measurements can be made up to 100 km with a more realistic limit being 80 km. It is clear from the graphs that an observation time of at least 10 seconds should be used.

## 6.2 Passive Resonant Absorption

This method is quite sensitive but requires a natural source. The strongest natural source is the solar disc. However, this method will be limited by the position of the sun in relation to a moving vehicle. This will impose short observational times on the measurement. The method does have the advantage that only one vehicle is required.

The minimum detectable optical depth is

$$\tau_{min} = \frac{\Delta T_{min}}{T_S \sec \phi} = \frac{2 \alpha}{\sqrt{t \Delta \nu}} \left( \frac{1}{10} + \frac{60}{T_S} \right) \tag{18}$$

for the 22.235 GHz line, and

$$\tau_{min} = \frac{\Delta T_{min}}{T_S \sec \phi} = \frac{2 \alpha}{\sqrt{t \Delta \nu}} \left( \frac{1}{10} + \frac{120}{T_S} \right) \tag{19}$$

for the 183.31 GHz line.

Table 4 of minimum detectable optical depths is obtained from equations 18 and 19. The same limiting values of $\alpha / \sqrt{t}$ as before are used.

Figures 6 and 7 are plotted with the limiting atmospheric optical depth values from Table 2 and the minimum detectable optical depths presented in Table 4. The figures show that a radiometer tuned to the 22.235 GHz line can measure water vapor up to 85 km under optimum conditions with 70 km being a more realistic limit. If,

Table 4: Minimum Detectable Optical Depths for Passive Resonant Absorption ($\Delta T_{min}/T_S \sec \phi$)

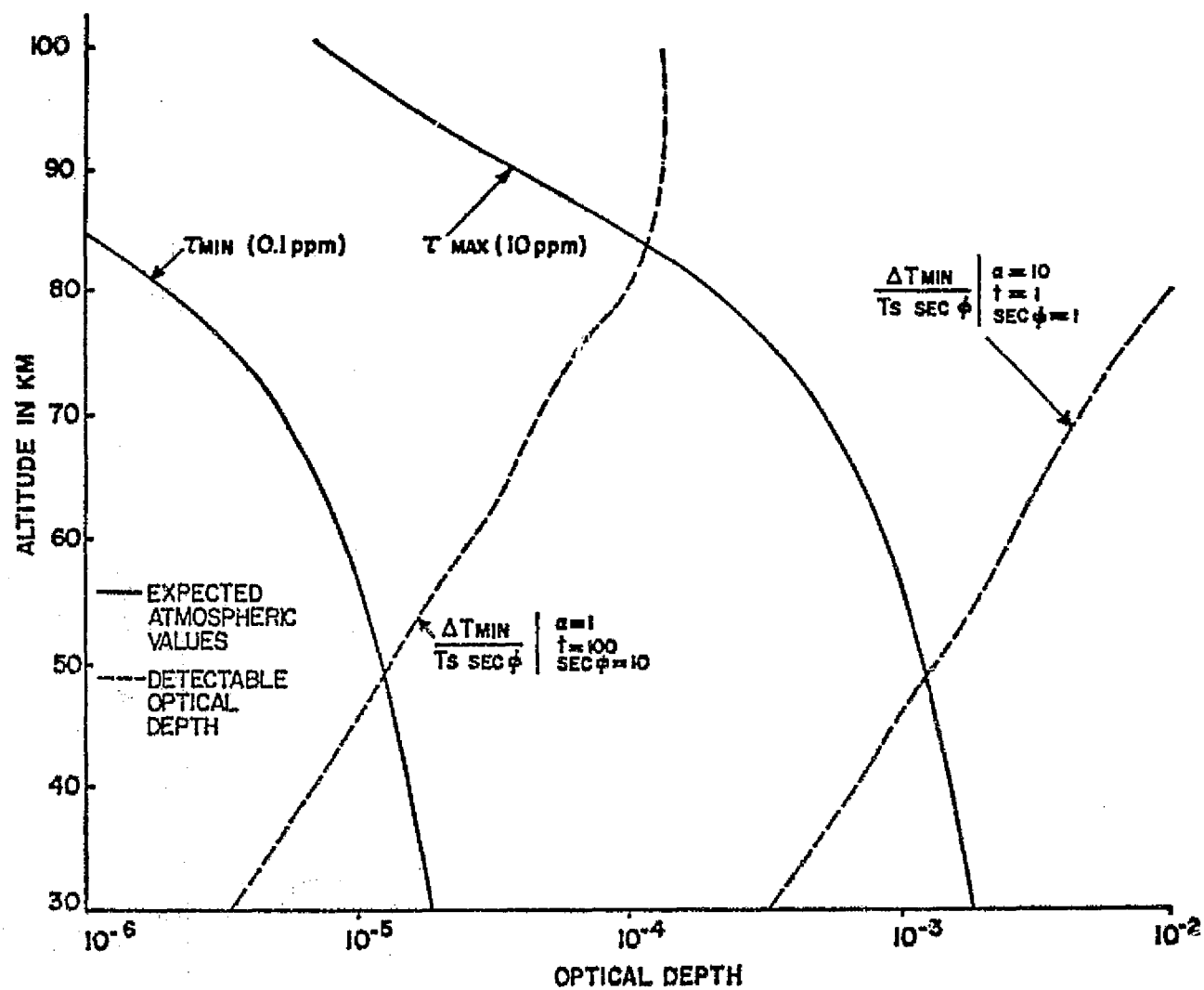| h | 22.235 GHz | | 183.31 GHz | |
|---|---|---|---|---|
| | $\dfrac{\alpha}{\sqrt{t}} = 0.1$ | $\dfrac{\alpha}{\sqrt{t}} = 10$ | $\dfrac{\alpha}{\sqrt{t}} = 0.1$ | $\dfrac{\alpha}{\sqrt{t}} = 10$ |
| 30 km | $3.4 \times 10^{-6}$ | $3.4 \times 10^{-4}$ | $3.8 \times 10^{-6}$ | $3.8 \times 10^{-4}$ |
| 40 km | $6.8 \times 10^{-6}$ | $6.8 \times 10^{-4}$ | $7.7 \times 10^{-6}$ | $7.7 \times 10^{-4}$ |
| 50 km | $1.3 \times 10^{-5}$ | $1.3 \times 10^{-3}$ | $1.5 \times 10^{-5}$ | $1.5 \times 10^{-3}$ |
| 60 km | $2.6 \times 10^{-5}$ | $2.6 \times 10^{-3}$ | $2.8 \times 10^{-5}$ | $2.8 \times 10^{-3}$ |
| 70 km | $4.4 \times 10^{-5}$ | $4.4 \times 10^{-3}$ | $4.2 \times 10^{-5}$ | $4.2 \times 10^{-3}$ |
| 80 km | $9.5 \times 10^{-5}$ | $9.5 \times 10^{-3}$ | $5.2 \times 10^{-5}$ | $5.2 \times 10^{-3}$ |
| 90 km | $1.3 \times 10^{-4}$ | $1.3 \times 10^{-2}$ | $5.3 \times 10^{-5}$ | $5.3 \times 10^{-3}$ |
| 100 km | $1.3 \times 10^{-4}$ | $1.3 \times 10^{-2}$ | $5.1 \times 10^{-5}$ | $5.1 \times 10^{-3}$ |
| 110 km | $1.2 \times 10^{-4}$ | $1.2 \times 10^{-2}$ | $4.8 \times 10^{-5}$ | $4.8 \times 10^{-3}$ |
| 120 km | $1.1 \times 10^{-4}$ | $1.1 \times 10^{-2}$ | $4.5 \times 10^{-5}$ | $4.5 \times 10^{-3}$ |

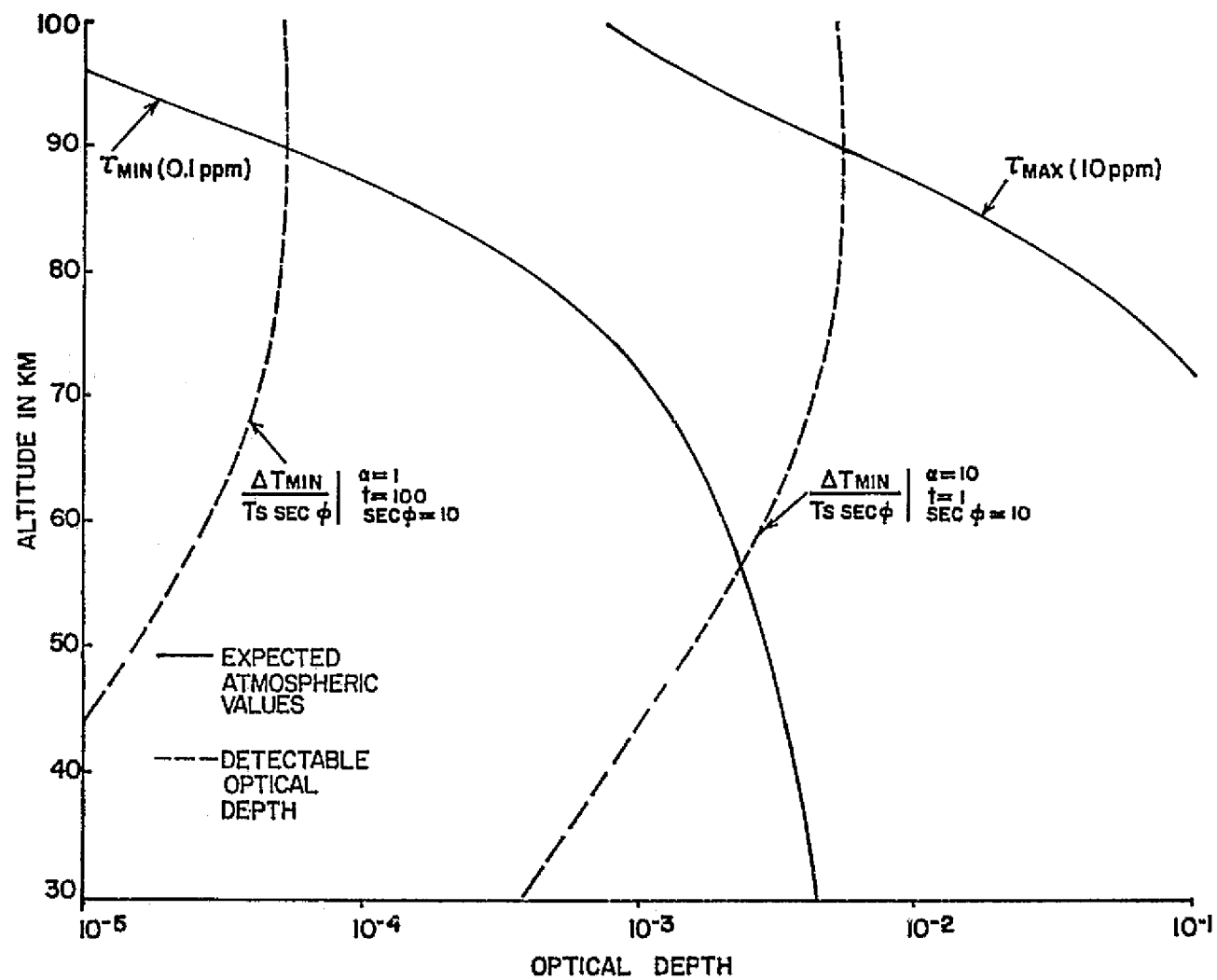Figure 6   22.235 GHz Passive Absorption Experiment

Figure 7  183.31 GHz Passive Absorption Experiment

however, the experiment is performed at 183.31 GHz, the measurement can be made all the way up to 100 km for the optimum conditions. However, this type of experiment should have an observation time of 10 seconds or shorter due to the relative movement of the source. Thus the upper limits of measurement would be less.

### 6.3 Active Resonant Absorption

This is the most versatile method. Global coverage is possible although an additional vehicle is required. The source can be a fixed frequency broad band source or a narrow band tuneable source. This method has the slight disadvantage that permission to operate the source must be obtained. However, the ability to control the source characteristics and the fact that this is a non-thermal source and thus will have less noise inherent in its output, make this experiment extremely attractive.

The minimum detectable optical depths for this case are

$$\tau_{min} = \frac{\Delta P_{min}}{P_S \sec \phi} = \frac{\alpha k \sqrt{\Delta \nu}}{\sqrt{t}} \left( \frac{120}{P_S} \right) \tag{20}$$

for the 22.235 GHz line and

$$\tau_{min} = \frac{\Delta P_{min}}{P_S \sec \phi} = \frac{\alpha k \sqrt{\Delta \nu}}{\sqrt{t}} \left( \frac{240}{P_S} \right) \tag{21}$$

for the 183.31 GHz line.

In the above expressions $P_S$ is given by equation 15 and has a value of $8.84 \times 10^{-14}$ Watts. From equations 20 and 21, the following table of minimum optical depths is obtained for both lines.

Table 5: Minimum Detectable Optical Depths for Active Absorption ($\Delta P_{min}/P_S \sec \phi$)

| | 22.235 GHz | | 183.31 GHz | |
|---|---|---|---|---|
| h | $\dfrac{\alpha}{\sqrt{t}} = 0.1$ | $\dfrac{\alpha}{\sqrt{t}} = 10$ | $\dfrac{\alpha}{\sqrt{t}} = 0.1$ | $\dfrac{\alpha}{\sqrt{t}} = 10$ |
| 30 km | $1.2 \times 10^{-5}$ | $1.2 \times 10^{-3}$ | $2.4 \times 10^{-5}$ | $2.4 \times 10^{-3}$ |
| 40 km | $5.8 \times 10^{-6}$ | $5.8 \times 10^{-4}$ | $1.2 \times 10^{-5}$ | $1.2 \times 10^{-3}$ |
| 50 km | $3.1 \times 10^{-6}$ | $3.1 \times 10^{-4}$ | $6.2 \times 10^{-6}$ | $6.2 \times 10^{-4}$ |
| 60 km | $1.5 \times 10^{-6}$ | $1.5 \times 10^{-4}$ | $3.2 \times 10^{-6}$ | $3.2 \times 10^{-4}$ |
| 70 km | $9.0 \times 10^{-7}$ | $9.0 \times 10^{-5}$ | $2.2 \times 10^{-6}$ | $2.2 \times 10^{-4}$ |
| 80 km | $4.2 \times 10^{-7}$ | $4.2 \times 10^{-5}$ | $1.7 \times 10^{-6}$ | $1.7 \times 10^{-4}$ |
| 90 km | $3.0 \times 10^{-7}$ | $3.0 \times 10^{-5}$ | $1.7 \times 10^{-6}$ | $1.7 \times 10^{-4}$ |
| 100 km | $3.1 \times 10^{-7}$ | $3.1 \times 10^{-5}$ | $1.8 \times 10^{-6}$ | $1.8 \times 10^{-4}$ |
| 110 km | $3.2 \times 10^{-7}$ | $3.2 \times 10^{-5}$ | $1.9 \times 10^{-6}$ | $1.9 \times 10^{-4}$ |
| 120 km | $3.5 \times 10^{-7}$ | $3.5 \times 10^{-5}$ | $2.0 \times 10^{-6}$ | $2.0 \times 10^{-4}$ |

From tables 2 and 5, figures 8 and 9 are plotted. Figure 8 shows that if a 22.235 GHz radiometer is used having a signal to noise ratio of 10 and an absorption time of 1 second, then water vapor can be measured up to 90 km if the true mixing ratio is 10 ppm. However, if the observation time is 100 seconds and the signal to noise ratio of 1 is sufficient, then water vapor can be measured above 100 km if the mixing ratio is 10 ppm and up to 90 km if the mixing ratio is 0.1 ppm. Figure 9 on the other hand shows that a great improvement results if the 183.31 GHz line is used. For a radiometer having a signal to noise ratio of 10 and an observation time of only 1 second, water vapor can be measured up to 85 km if the mixing ratio is .1 ppm and above 100 km if the mixing ratio is 10 ppm. A measurement made with a radiometer having a signal to noise ratio of 1 and an observation time = 100 seconds, can detect and measure water vapor above 100 km even if the mixing ratio is only .1 ppm. Thus this measurement seems to be very feasible. An experiment having only 1 second for observing time should give quite accurate results. The sensitivity of the active experiment can be increased by increasing the power of the transmitter. This will then move the $\Delta P_{min}/P_S$ curves to the left. However, there is a major problem to be considered in this technique.

At high power levels transitions among the molecular states are induced at a rate that is not negligible compared with the collision rate, thus invalidating the assumption of thermal equilibrium for the specific rotational state (Karplus et al., 1948). The absorption line is then broadened as the power level is increased with a corresponding decrease in the peak resonant cross section. The energy absorbed per unit volume will then reach a saturation level and thus perturb the
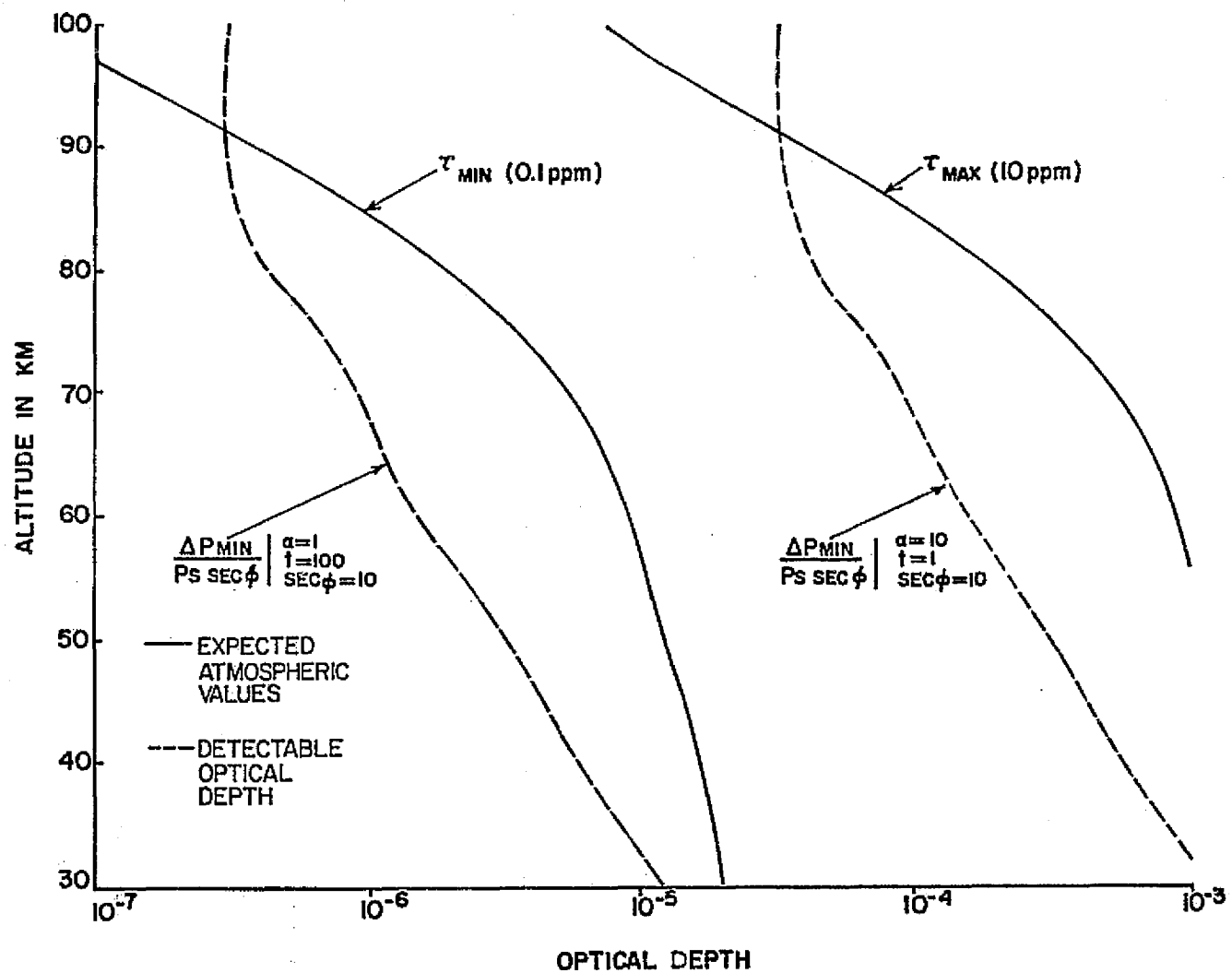
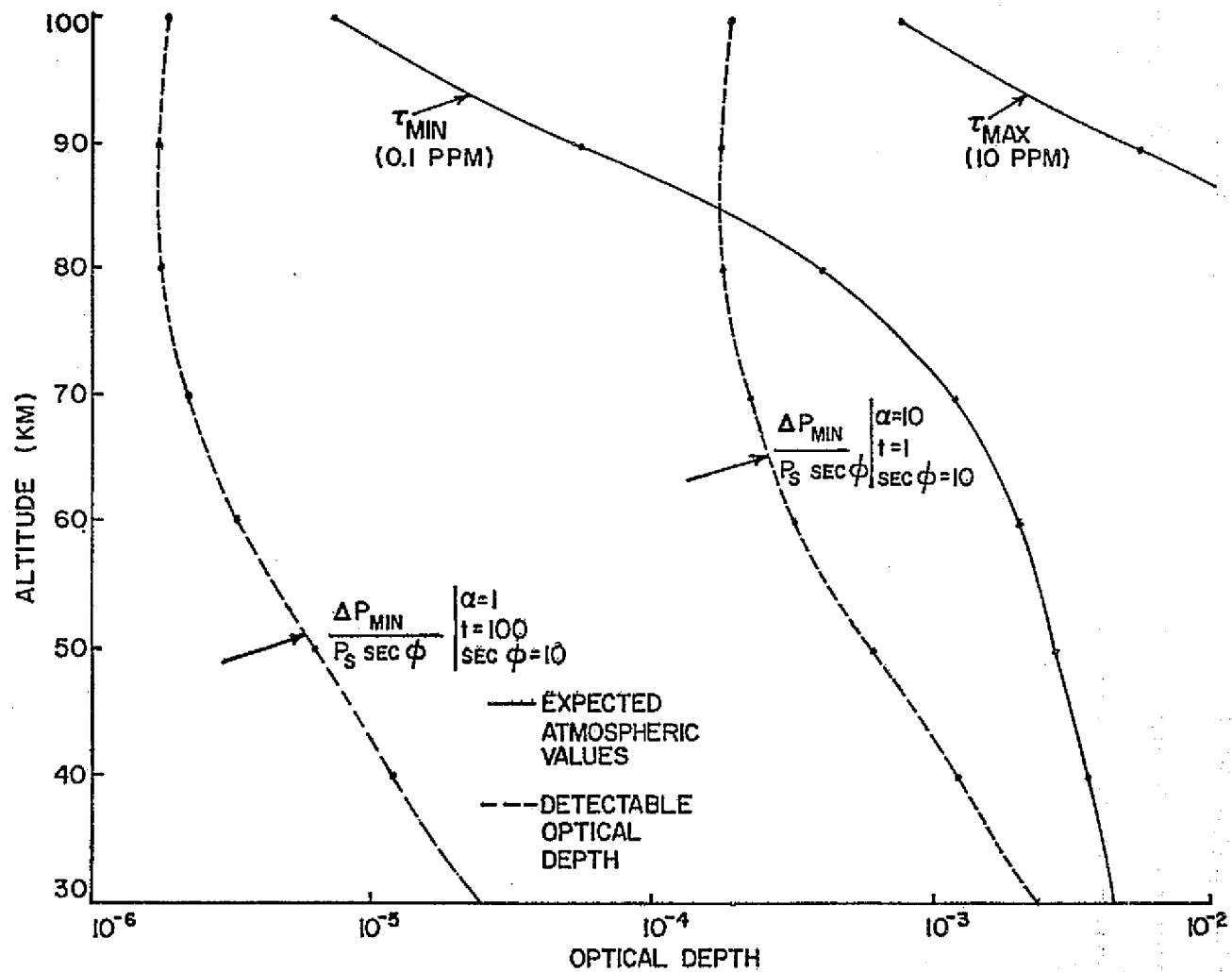Figure 8   22.235 GHz Active Absorption Experiment

Figure 9  183.31 GHz Active Absorption Experiment

31

measurement. This means that the level of power used to excite the medium may be extremely critical and thus this possibility should be examined more closely. This situation is looked at in Appendix D and it appears that saturation effects will not be important for stratospheric measurements unless the power density exceeds 19 millwatts/$m^2$.

# CHAPTER VII

## CONCLUSIONS

The distribution of water vapor in the upper atmosphere must be known if one is to obtain a better understanding of upper atmospheric physical processes. This will be necessary to assess the impact of artificially introduced products on the photochemical and radiational balances of the upper atmosphere. Water vapor may also be responsible for hydrated ions and noctilucent clouds. Thus a measurement of stratospheric and mesospheric water vapor is of considerable importance to the scientific community.

Past measurements of water vapor have been limited to about 30 km due to the lack of sufficiently sensitive instruments. However, due to state of the art advances in low noise receiver development (the Schottky barrier diode), weak signals from stratospheric water vapor can now be measured.

The results of this study show that using an occultation experiment, water vapor concentrations as low as 0.1 ppm can be detected above 30 km and with sufficient instrument resolution, up to' and above 100 km. The 22.235 GHz line of water vapor can only be used for an active absorption experiment, if measurements to 90 km are desired (see Table 6). However, the water vapor line at 183.31 GHz will enable measurements to be made up to 80 km using the least sensitive mode of operation (passive emission). This mode also has the advantage that a radiation source is not required and therefore the experiment will be greatly simplified and more nearly continuous measurements can be made. The active absorption experiment might offer the advantage of probing the water vapor line shape more

Table 6: Upper Altitude Limits of Water Vapor Measurement

| Mode Active Absorption (10 Milliwatt Source) | | Mode Passive Absorption (Solar Disc) | | Mode Passive Emission (Atmospheric Temperature) | | Radiometer Parameters | Radiometer Parameters |
|---|---|---|---|---|---|---|---|
| Frequency GHz 183.31 | Frequency GHz 22.235 | Frequency GHz 183.31 | Frequency GHz 22.235 | Frequency GHz 183.31 | Frequency GHz 22.235 | | |
| Below 85 km | Below 30 km | Below 55 km | Below 30 km | Below 40 km | Below 30 km | Min. Water Vapor Mixing Ratio — 0.1 ppm | $\alpha = 10,\ t = 1$ sec |
| Above 100 km | Above 90 km | Above 90 km | Above 50 km | Above 80 km | Above 35 km | Max. Water Vapor Mixing Ratio — 10 ppm | $\alpha = 10,\ t = 1$ sec |
| Above 100 km | Above 90 km | Above 90 km | Above 50 km | Above 80 km | Above 35 km | Min. Water Vapor Mixing Ratio — 0.1 ppm | $\alpha = 1,\ t = 100$ sec |
| Above 100 km | Above 100 km | Above 100 km | Above 85 km | Above 100 km | Above 75 km | Max. Water Vapor Mixing Ratio — 10 ppm | $\alpha = 1,\ t = 100$ sec |

accurately, but the emission experiment performed at 183.31 GHz appears to be the simplest, least expensive, and most desirable experiment.

The experiment should now be examined using a computer simulation. The radiative transfer problem will be examined in much more detail especially the effects of combined pressure and Doppler broadening on the (signal) line shape. Various atmospheric water vapor models will be simulated to determine the relative effect on the signal. The orbital and spatial motions of a vehicle will be studied as to the restrictions they place on a measurement. The amount of water vapor in the viewing path will be varied in order to determine the degree of sensitivity of the signal to various regions along the viewing path. The measurement should also be modeled to see how far off the line center a measurement can still be made. Comparisons between several vehicles and various types of measurements will then be drawn. This study will provide the theoretical background on which to base future experiments.

# APPENDIX A

## WATER VAPOR ABSORPTION COEFFICIENTS

The absorption coefficient for the pressure broadened 22.235 GHz line is given by (Croom, 1965)

$$K_a\ (\nu,\ \Delta\nu,\ T,\ N)\ =\ 1.05 \times 10^{-28}\ \frac{N\nu^2}{T^{5/2}}\ \exp\ (-644/T).$$

$$\left[ \frac{\Delta\nu}{(\nu - \nu o)^2 + \Delta\nu^2}\ +\ \frac{\Delta\nu}{(\nu + \nu o)^2 + \Delta\nu^2} \right]$$

$$+\ 1.52 \times 10^{-52}\ \frac{N\nu^2 \Delta\nu}{T^{3/2}}\ \mathrm{cm}^{-1} \tag{A.1}$$

where

N   is the number density of water vapor molecules in $\mathrm{cm}^{-3}$

$\nu$   is the frequency in Hz

and

T   is the kinetic temperature in $^\circ$K

The absorption coefficient for the pressure broadened 183.31 GHz line is given as (Croom, 1965)

$$K_a\ (\nu,\ \Delta\nu,\ T,\ N)\ =\ 6.46 \times 10^{-29}\ \frac{N\nu^2}{T^{5/2}}\ \exp\ (-200/T).$$

$$\left[ \frac{\Delta\nu}{(\nu - \nu o)^2 + \Delta\nu^2}\ +\ \frac{\Delta\nu}{(\nu + \nu o)^2 + \Delta\nu^2} \right]$$

$$+ 1.8 \times 10^{-52} \frac{N \nu^2 \Delta\nu}{T^{3/2}} \, cm^{-1} \tag{A.2}$$

In previous atmospheric work (Croom, 1965) absorption calculations have been simplified by assuming a pressure broadened line shape for all altitudes. This has the effect of assuming the same line shape for Doppler broadening as for pressure broadening. Above 70 km where Doppler broadening becomes dominant, this is in error since Doppler broadening has a different line shape (Longbothum, 1974). The error, however, appears to be slight according to Croom (1965) and thus the only account of Doppler broadening in the calculations is through the line width constant $\Delta\nu$. When both the effects of Doppler broadening and pressure broadening are appreciable (above 70 km), the value of $\Delta\nu$ is given approximately by (Croom, 1965).

$$\Delta\nu \cong (\Delta\nu_p{}^2 + \Delta\nu_d{}^2)^{1/2} \tag{A.3}$$

The pressure broadening is given by (Croom, 1965)

$$\Delta\nu_p = 2.62 \times 10^9 \frac{\left(\frac{P}{1013.25}\right)}{\left(\frac{T}{318}\right)^{0.625}} (1 + 0.0046 \, \rho) \quad Hz \tag{A.4}$$

where

P   is the total atmospheric pressure in mb

$\rho$   is the density of the water vapor in gm m$^{-3}$

T   is the kinetic temperature in $^{\circ}$K

The Doppler broadening is given by (Croom, 1965).

$$\Delta\nu_d = 3.58 \times 10^{-7} \sqrt{\frac{T}{M}} \, \nu_o \quad Hz \tag{A.5}$$

where M is the molecular weight of the gas.

For water vapor (M = 18) the expression for Doppler broadening is

$$\Delta \nu_d \;=\; 8.45 \times 10^{-8} \; \sqrt{T} \; \nu_o \quad Hz \qquad\qquad (A.6)$$

APPENDIX B

## DERIVATION OF THE EQUATION OF SENSITIVITY FOR A MICROWAVE RADIOMETER VIEWING A THERMAL SOURCE

Consider the total power superheterodyne receiver (see figure 10) monitoring a thermal noise source such as the solar disc. For this case $\Delta T$, the input signal will be broadband random noise. The two sided power spectral density of $V_{IN}$ will be (Tiuri, 1964)

$$\Phi_{IN}(j\omega) = \frac{1}{2} k (T_A + T_R + \Delta T) = \frac{1}{2} k (T_{SN} + \Delta T)$$

(B. 1)

The noise input then will be band limited by the bandwidth of the tuned RF and IF amplifiers. The bandwidth of the IF amplifier is generally smaller and thus has the dominant effect. The bandwidth is given by (Burdic, 1968)

$$B_{HF} = \frac{\left[\int_0^\infty |A(j\omega)|^2 \, df\right]^2}{\int_0^\infty |A(j\omega)|^4 \, df}$$

(B. 2)

where $\omega = 2\pi f$

After the RF and IF amplifiers, the spectral density (power) is obtained from equation (1) by multiplying it with the power amplification ratio $|A(j\omega)|^2$.
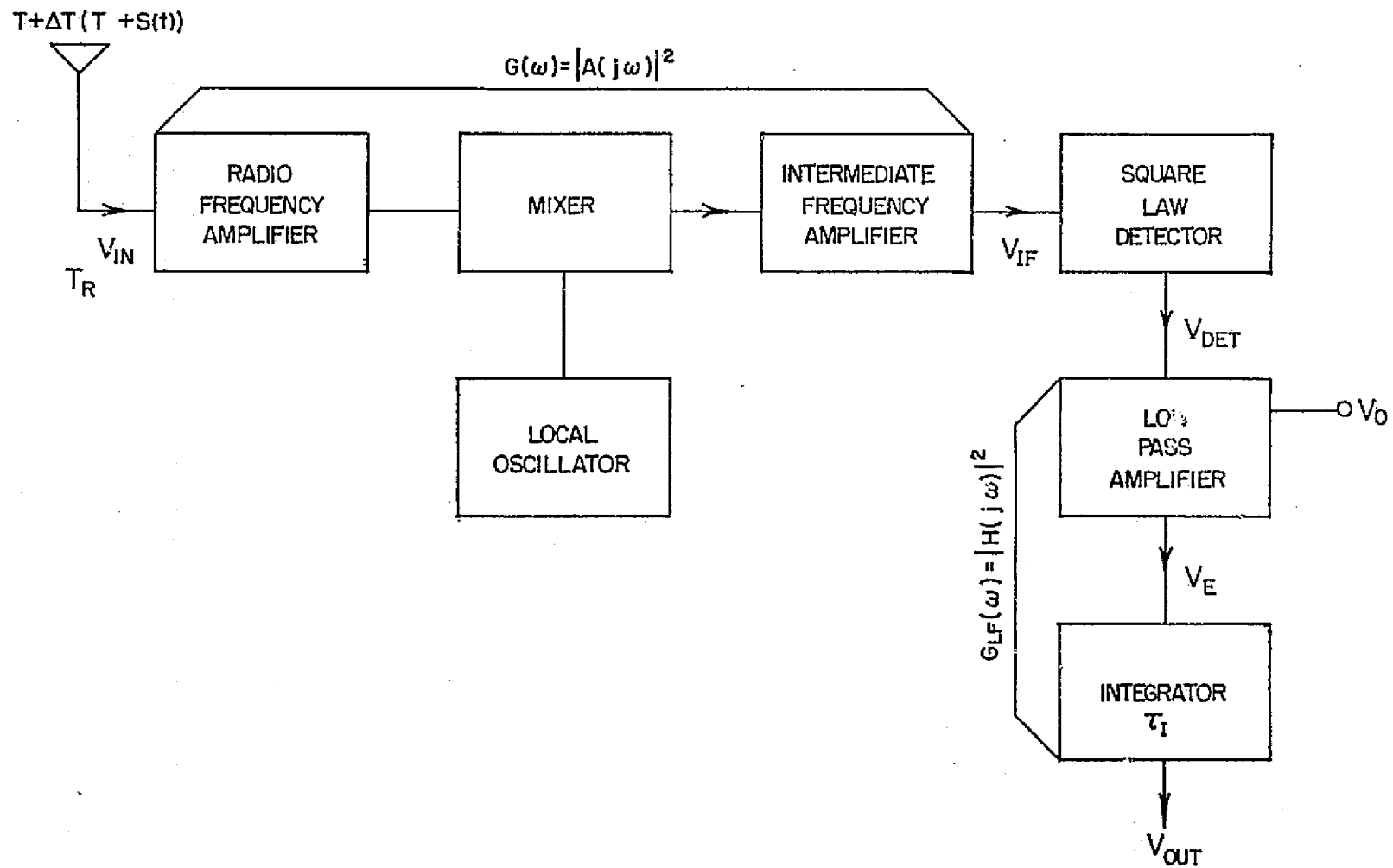
Thus

$T+\Delta T\,(T\ +S(t))$

$G(\omega)=\left|A(\,j\,\omega)\right|^{2}$

$T_R$

$V_{IN}$

RADIO
FREQUENCY
AMPLIFIER

MIXER

LOCAL
OSCILLATOR

INTERMEDIATE
FREQUENCY
AMPLIFIER

$V_{IF}$

SQUARE
LAW
DETECTOR

$V_{DET}$

$G_{LF}(\omega)=\left|H(\,j\,\omega)\right|^{2}$

LOW
PASS
AMPLIFIER

$\circ\,V_0$

$V_E$

INTEGRATOR
$\tau_I$

$V_{OUT}$

Figure 10  Total Power Superheterodyne Receiver

$$\Phi_{IF}(j\omega) = \tfrac{1}{2}k(T_{SN} + \Delta T)\left|A(j\omega)\right|^2 \tag{B.3}$$

If we assume that the input signal is gaussian white noise with zero mean and autocorrelation function

$$R_{IF}(\tau) = \int_{-\infty}^{\infty} e^{j\omega\tau}\,\Phi_{IF}(j\omega)\,df \tag{B.4}$$

Then the output from the square law detector will be given by (Thomas, 1969)

$$R_{Det}(\tau) = R_{IF}^2(o) + 2R_{IF}^2(\tau) \tag{B.5}$$

From this

$$\Phi_{Det}(j\omega) = \tfrac{1}{2\pi}\int_{-\infty}^{\infty} e^{-j\omega\tau}R_{Det}(\tau)\,d\tau$$

$$= 2\pi\delta(\omega)R_{IF}^2(o) + \tfrac{1}{\pi}\int_{-\infty}^{\infty}\Phi_{IF}(ju)\,\Phi_{IF}(j\omega - ju)\,du \tag{B.6}$$

The first term is the D. C. component resulting from the rectified signal and system noise. The second term is the convolution of the input spectrum.

The D. C. term constitutes the signal power that is measured. This is

$$\Phi_{Det}^{D.C.}(j\omega) = 2\pi\,\delta(\omega)\left[\int_{-\infty}^{\infty}\Phi_{IF}(j\omega)\,df\right]^2 \tag{B.7}$$

The average D. C. power delivered to a one ohm resistor in the low pass filter is given by

$$\overline{P}_{D.C.} = \overline{V_{Det}^2} = \int_{-\infty}^{\infty} \Phi_{Det}^{D.C.}(j\omega)\, df$$

(B. 8)

Thus

$$\overline{V_{Det}^2} = \frac{1}{2\pi} \int_{-\infty}^{\infty} 2\pi\, \phi(\omega) \left[ \int_{-\infty}^{\infty} \Phi_{IF}(j\omega)\, df \right]^2 d\omega$$

$$= \left[ \int_{-\infty}^{\infty} \Phi_{IF}(j\omega)\, df \right]^2 = \left[ \overline{V}_{Det} \right]^2$$

(B. 9)

or

$$\overline{V}_{Det} = E[V_{Det}] = \int_{-\infty}^{\infty} \Phi_{IF}(\omega)\, df$$

$$= \int_{-\infty}^{\infty} \frac{1}{2}k\,(T_{SN} + \Delta T)\, |A(j\omega)|^2\, df$$

(B. 10)

At the first stage of the low pass filter, a voltage

$$V_o = -\frac{1}{2}k\, T_{SN} \int_{-\infty}^{\infty} |A(j\omega)|^2 df$$

(B. 11)

is injected to cancel the D. C. component due to system noise. The difference is a measure of the signal noise temperature.

$$\overline{V}_e = E[V_e] = \tfrac{1}{2}k.\Delta T \int_{-\infty}^{\infty} |A(j\omega)|^2 df \tag{B.12}$$

This represents the signal going into the integrator. The low pass filter will remove most of the random fluctuations. The variance (mean squared normalized power) of the noise fluctuations is given by

$$\sigma_{out}^2 = E[V_{out}^2] - E^2[V_{out}]$$

$$= \int_{-\infty}^{\infty} df |H(j\omega)|^2 \tfrac{1}{4\pi}k^2(T_{SN} + \Delta T)^2 \int_{-\infty}^{\infty} |A(ju)|^2 ,$$

$$|A(j\omega - ju)|^2 du$$

$$= \int_{-\infty}^{\infty} |H(j\omega)|^2 \tfrac{1}{2} k^2(T_{SN} + \Delta T)^2 df \int_{-\infty}^{\infty} |A(ju)|^2 ,$$

$$|A(j\omega - ju)|^2 \frac{du}{2\pi} \tag{B.13}$$

The post detection bandwidth is given by (Carlson, 1968)

$$B_{LF} = \int_{0}^{\infty} \left| \frac{H(j\omega)}{H(o)} \right|^2 df \tag{B.14}$$

Since this bandwidth is much smaller than $B_{HF}$, $\omega$ may be set equal to zero in equation (13). The average D. C. $V_{out}$ is given by

$$E[V_{out}] = E[V_e] |H(o)| \tag{B.15}$$

If equation (13) is divided by this relation (equation 15), then the relative deviation is obtained.

$$\sigma_{out}^{*} \;=\; \frac{\sigma_{out}}{E[V_{out}]}$$

$$=\; \frac{\left[ \int_{-\infty}^{\infty} |H(j\omega)|^{2}\, \frac{k^{2}}{2}\, (T_{SN} + \Delta T)^{2}\, df \int_{-\infty}^{\infty} |A(j\omega)|^{4}\, df \right]^{1/2}}{|H(o)| \int_{-\infty}^{\infty} \frac{k}{2}\, \Delta T\, |A(j\omega)|^{2}\, df}$$

$$=\; \left[ B_{LF}\; 2\; \left[ \frac{T_{SN} + \Delta T}{\Delta T} \right]^{2}\; B_{HF}^{-1} \right]^{1/2} \tag{B.16}$$

or

$$\sigma_{out}^{*} \;=\; \frac{\sigma_{out}}{E[V_{out}]} \;=\; \frac{T_{SN} + \Delta T}{\Delta T}\; \sqrt{\frac{2 B_{LF}}{B_{HF}}} \tag{B.17}$$

For any physical system, there exists an uncertainty principle between bandwidth and risetime given by (Carlson, 1968)

$$B_{LF}\, \tau_{I} \;\geq\; \tfrac{1}{2} \tag{B.18}$$

Thus for a perfect integrator with integration time $\tau_{I}$,

$$B_{LF} \;=\; \frac{1}{2\, \tau_{I}} \tag{B.19}$$

and

$$\sigma^{*}_{out} = \frac{T_{SN} + \Delta T_{min}}{\Delta T_{min}} \sqrt{\frac{1}{B_{HF} \tau_I}} \tag{B.20}$$

The sensitivity of the radiometer is defined as the signal which will give a D. C. output voltage equal to or greater than the effective value of the output fluctuations due to the system noise (Tiuri, 1964). Thus if we consider an output signal to noise voltage ratio $\alpha$, then the equation for sensitivity is

$$\frac{\Delta T_{min}}{T_{SN} + \Delta T_{min}} = \alpha \sqrt{\frac{1}{B_{HF} \tau_I}} \tag{B.21}$$

This can be solved for $\Delta T_{MIN}$

$$\Delta T_{Min} = \frac{\alpha \, T_{SN}}{\sqrt{B_{HF} \tau_I} - \alpha} \tag{B.22}$$

There is one problem with the total power receiver. The receiver can not distinguish between the change in signal power and the change in receiver gain. Thus it is very important to stabilize the gain of the receiver. The best receiver for this purpose has been that of Dicke (1946) in which he introduced a modulation of signal input in order to eliminate the fluctuations induced by receiver instabilities. The input of the receiver is switched between the antenna and a reference noise power. The rate of switching is at

such a frequency that the amplitude of gain fluctuations is negligible. The amplitude of the signal then may be determined by means of a coherent detector which is driven at the same switching frequency. However since the signal is connected to the receiver only half of the time, the sensitivity of the Dicke receiver is only one half as high as the total power receiver thus

$$\Delta T_{Min} = \frac{2T_{SN} \, \alpha}{\sqrt{B_{HF} \, \tau_I} - \alpha} \qquad (B.23)$$

For practical bandwidths $B_{HF}$, this will reduce to

$$\Delta T_{Min} = \frac{2 \, T_{SN} \, \alpha}{\sqrt{B_{HF} \, \tau_I}} \qquad (B.24)$$

# APPENDIX C

## DERIVATION OF THE EQUATION OF SENSITIVITY FOR A MICROWAVE RADIOMETER VIEWING A NON-THERMAL SOURCE

Consider the total power superheterodyne receiver (see figure 10) monitoring a continuous wave signal from an oscillator. For this case the signal input to the receiver will be

$$x(t) = s(t) + n(t) \tag{C.1}$$

where $s(t) = A \cos(\omega_o t + \Theta)$ and $n(t)$ represents the random background and receiver noise. A is a constant and $\Theta$ is a random variable uniformly distributed over the interval $0 \leq \Theta \leq 2\pi$. For wide sense stationary noise and signal, the autocorrelation functions are (Thomas, 1969)

$$R_s(\tau) = \frac{A^2}{2} \cos \omega_o \tau \tag{C.2}$$

and

$$R_n(\tau) = \frac{1}{2} k T_{SN} \delta(\tau) \tag{C.3}$$

From these the power spectral density can be obtained

$$\Phi_{In}^{noise}(j\omega) = \frac{1}{2} k T_{SN} \tag{C.4}$$

$$\Phi_{In}^{signal}(j\omega) = \frac{A^2 \pi}{2} [\delta(\omega - \omega_o) + \delta(\omega + \omega_o)] \tag{C.5}$$

After the RF and IF amplifiers, the spectral densities are obtained from equations (4) and (5) by multiplying them with the power amplification ratio $|A(j\omega)|^2$.

$$\Phi_{IF}^{noise}(j\omega) = \frac{1}{2} k\, T_{SN}\, |A(j\omega)|^2 \tag{C.6}$$

and

$$\Phi_{IF}^{signal}(j\omega) = \frac{A^2 \pi}{2} \left[\delta(\omega - \omega_o) + \delta(\omega + \omega_o)\right]\, |A(j\omega)|^2 \tag{C.7}$$

Then the autocorrelation functions at the input of the square law detector are

$$R_{IF}^{noise}(\tau) = \frac{k\, T_{SN}}{4\pi} \int_{-\infty}^{\infty} |A(j\omega)|^2\, e^{j\omega\tau}\, d\omega \tag{C.8}$$

and

$$R_{IF}^{signal}(\tau) = \frac{A^2}{4} \int_{-\infty}^{\infty} \left[\delta(\omega - \omega_o) + \delta(\omega + \omega_o)\right] \cdot$$

$$|A(j\omega)|^2 e^{j\omega\tau} d\omega = \frac{A^2}{4} \left[|A(j\omega_o)|^2 e^{j\omega_o\tau}\right.$$

$$\left. + |A(-j\omega_o)|^2 e^{-j\omega_o\tau}\right] = \frac{A^2}{2} |A(j\omega_o)|^2 \cos\omega_o\tau \tag{C.9}$$

If we assume that the input noise is gaussian with zero mean and auto-correlation function as given above, then the output from the square

law detector will be

$$R_{Det}^{s+n}(\tau) = R_{Det}^{n \times n}(\tau) + R_{Det}^{s \times n}(\tau) + R_{Det}^{s \times s}(\tau) \tag{C.10}$$

where the interaction of the noise with itself is (Thomas, 1969)

$$R_{Det}^{n \times n}(\tau) = R_{Det}^{n^2}(\tau) = \left(R_{IF}^{noise}(o)\right)^2 + 2\left(R_{IF}^{noise}(\tau)\right)^2$$

$$= \sigma_n^4 + 2\left[\frac{kT_{SN}}{4\pi} \int_{-\infty}^{\infty} |A(j\omega)|^2 e^{j\omega\tau} d\omega\right]^2 \tag{C.11}$$

where

$$\sigma_n^2 = R_{IF}^n(o) = \frac{kT_{SN}}{2} \int_{-\infty}^{\infty} |A(j\omega)|^2 df \tag{C.12}$$

The interaction of the noise with the signal is given by (Thomas, 1969)

$$R_{Det}^{s \times n}(\tau) = 4R_{IF}^s(\tau) R_{IF}^n(\tau) + 2R_{IF}^s(o) R_{IF}^n(o)$$

$$= 2\sigma_s^2 \sigma_n^2 + 4\sigma_s^2 \cos\omega_o\tau \left[\frac{kT_{SN}}{4\pi} \int_{-\infty}^{\infty}\right.$$

$$\left. \cdot |A(j\omega)|^2 e^{j\omega\tau} d\omega\right] \tag{C.13}$$

where

$$\sigma_s^2 = R_{IF}^s (o) = \frac{A^2 \, |A(j\,\omega_o)|^2}{2}$$

(C. 14)

The interaction of the signal with itself is given by

$$R_{Det}^{s \times s} (\tau) = R_{Det}^{s^2} (\tau) = E\left\{s^2(t) \cdot s^2(t+\tau)\right\}$$

(C. 15)

The signal at the input of the detector has been modified by its passage through the RF and IF amplifiers. Thus the signal at the input of the square law detector is given by

$$s(t) = A \, |A(j\omega)| \, \cos\left[\omega_o t + \Theta + \phi(\omega)\right]$$

$$= A_1 \cos\left[\omega_o t + \gamma\right]$$

(C. 16)

where $\gamma$ is still uniformly distributed over the interval $o \leq \gamma \leq 2\pi$. Then the autocorrelation function of the detector output is

$$R_{Det}^{s^2} (\tau) = A_1^4 \left\{\cos^2(\omega_o t + \gamma)\cos^2\left[\omega_o(t+\tau) + \gamma\right]\right\}$$

$$= A_1^4 \left[\frac{1}{4} + \frac{1}{8} \cos 2\omega_o \tau\right]$$

(C. 17)

Thus the square law detector output autocorrelation function is

$$R_{Det}^{s+n}(\tau) = \left(\sigma_s^2 + \sigma_n^2\right)^2 + \frac{\sigma_s^4}{2} \cos 2\omega_o \tau$$

$$+ 2 \left[\frac{k T_{SN}}{4\pi} \int_{-\infty}^{\infty} |A(j\omega)|^2 e^{j\omega\tau} d\omega\right]^2$$

$$+ 4\sigma_s^2 \cos\omega_o \tau \left[\frac{k T_{SN}}{4\pi} \int_{-\infty}^{\infty} |A(j\omega)|^2 e^{j\omega\tau} d\omega\right] \tag{C.18}$$

The spectral density at the output of the square law detector will be

$$\Phi_{Det}^{n+s}(j\omega) = \Phi_{Det}^{s \times s}(j\omega) + \Phi_{Det}^{s \times n}(j\omega) + \Phi_{Det}^{n \times n}(j\omega) \tag{C.19}$$

where

$$\Phi_{Det}^{n \times n}(j\omega) = \int_{-\infty}^{\infty} R_{Det}^{n \times n}(\tau) e^{-j\omega\tau} d\tau = 2\pi \delta(\omega) \left(R_{IF}^n(o)\right)^2$$

$$+ \frac{1}{\pi} \int_{-\infty}^{\infty} \Phi_{IF}^n(ju) \Phi_{IF}^n(j\omega - ju) du = 2\pi \sigma_n^4 \delta(\omega)$$

$$+ \frac{1}{\pi} \int_{-\infty}^{\infty} \left(\frac{k T_{SN}}{2}\right)^2 |A(j\omega)|^2 |A(j\omega - ju)|^2 du \tag{C.20}$$

Then

$$\Phi_{Det}^{s \, x \, n}(j\omega) = \int_{-\infty}^{\infty} R_{Det}^{s \, x \, n}(\tau) \, e^{-j\omega\tau} \, d\tau$$

$$= 4\pi \; \delta(\omega) \; R_{IF}^{n}(o) \; R_{IF}^{s}(o) \; + \frac{2}{\pi} \int_{-\infty}^{\infty} \Phi_{IF}^{n}(ju) \; \Phi_{IF}^{s}$$

$$(j\omega - ju) \, du = 4\pi \; \sigma_n^2 \; \sigma_s^2 \; \delta(\omega)$$

$$+ \frac{2}{\pi} \int_{-\infty}^{\infty} \frac{k \, T_{SN}}{2} \, |A(j\omega - ju)|^2 \, \frac{A^2 \, \pi}{2} \cdot$$

$$|A(ju)|^2 \, [\, \delta(u - \omega_o) + \delta(u + \omega_o)] \, du$$

$$= 4\pi \; \sigma_n^2 \; \sigma_s^2 \; \delta(\omega) \; + \; \sigma_s^2 \, (k \, T_{SN}) \cdot$$

$$[\, |A(j\omega - j\omega_o)|^2 + |A(j\omega + j\omega_o)|^2] \tag{C.21}$$

and

$$\Phi_{Det}^{s \, x \, s}(j\omega) = \int_{-\infty}^{\infty} R_{Det}^{s^2}(\tau) \, e^{-j\omega\tau} \, d\tau$$

$$= 2\pi \; \sigma_s^4 \; \delta(\omega) + \frac{\pi}{2} \; \sigma_s^4 \quad [\, \delta(\omega - 2\omega_o) + \delta(\omega + 2\omega_o)] \tag{C.22}$$

Thus the square law detector output spectral density becomes

$$\Phi_{Det}^{s+n} (j\omega) = 2\pi \delta(\omega) [ \sigma_s^2 + \sigma_n^2 ]^2 + \frac{\pi}{2} \sigma_s^4 \cdot$$

$$[\delta(\omega - 2\omega_o) + \delta(\omega + 2\omega_o)] + \frac{1}{\pi} \int_{-\infty}^{\infty} \left( \frac{kT_{SN}}{2} \right)^2 \cdot$$

$$|A(ju)|^2 |A(j\omega - ju)|^2 du + 2\sigma_s^2 \left( \frac{kT_{SN}}{2} \right) \cdot$$

$$\left[ |A(j\omega - j\omega_o)|^2 + |A(j\omega + j\omega_o)|^2 \right] \tag{C.23}$$

The first term in equation (23) is the D.C. component resulting from the rectified signal and system noise. The average value of this term is

$$\overline{V}_{Det} = E\{V_{Det}\} = \sigma_s^2 + \sigma_n^2 \tag{C.24}$$

If a voltage $V_o$ is injected into the first stage of the low pass filter where

$$V_o = -\sigma_n^2 \tag{C.25}$$

then the D.C. voltage due to noise temperature will be canceled and the difference $V_e$ is a measure of the signal temperature where

$$\overline{V}_e = E\{V_e\} = \sigma_s^2 \tag{C.26}$$

The receiver output spectral density is given by

$$\Phi_{out}^{s+n} (j\omega) = \Phi_{Det}^{s+n} (j\omega) \; |H(j\omega)|^2 \tag{C.27}$$

However, the low pass filter will pass only those frequency components in the vicinity of zero. Thus the output spectral density is

$$\Phi_{out}^{s+n} (j\omega) = \left[ 2\pi \sigma_s^4 \delta(\omega) + 2 \int_{-\infty}^{\infty} \frac{kT_{SN}}{2}^2 |A(j\omega)|^4 \, df \right.$$

$$\left. + 2 \sigma_s^2 |A(j\omega_0)|^2 (kT_{SN}) \right] |H(j\omega)|^2 \tag{C.28}$$

or using

$$B_{HF} \equiv \frac{\left[ \int_{-\infty}^{\infty} |A(j\omega)|^2 \, df \right]^2}{\int_{-\infty}^{\infty} |A(j\omega)|^4 \, df} \tag{C.29}$$

one can write

$$\Phi_{out}^{s+n} (j\omega) = |H(j\omega)|^2 \left\{ 2\pi \sigma_s^4 \delta(\omega) + \frac{2\sigma_n^4}{B_{HF}} + 2\sigma_s^2 \cdot \right.$$

$$\left. |A(j\omega_0)|^2 (kT_{SN}) \right\} \tag{C.30}$$

Another definition of noise bandwidth is (Thomas, 1969)

$$B_{HF} = \int_{-\infty}^{\infty} \left| \frac{A(j\omega)}{A(j\omega_0)} \right|^2 \, df \tag{C.31}$$

This can be used to write

$$|A(j\omega_o)|^2 = \frac{1}{B_{HF}} \int_{-\infty}^{\infty} |A(j\omega)|^2 \, df$$

(C.32)

and thus equation (30) can be written as

$$\Phi_{out}^{s+n}(j\omega) = |H(j\omega)|^2 \left\{ 2\pi\sigma_s^4 \delta(\omega) + \frac{2\sigma_n^4}{B_{HF}} + \frac{4\sigma_s^2\sigma_n^2}{B_{HF}} \right\}$$

(C.33)

The output autocorrelation function is then

$$R_{out}^{s+n}(\tau) = \frac{1}{2\pi} \int_{-\infty}^{\infty} \Phi_{out}^{s+n}(j\omega) \, e^{j\omega\tau} \, d\omega =$$

$$\sigma_s^4 |H(o)|^2 + \frac{1}{2\pi} \int_{-\infty}^{\infty} \frac{2\sigma_n^4}{B_{HF}} |H(j\omega)|^2 \, e^{j\omega\tau} \, d\omega$$

$$+ \frac{1}{2\pi} \int_{-\infty}^{\infty} 4\sigma_s^2\sigma_n^2 \frac{|H(j\omega)|^2}{B_{HF}} \, e^{j\omega\tau} \, d\omega$$

(C.34)

The average or D. C. value of the output is

$$\overline{V}_{out} = E\{V_{out}\} = \overline{V}_e \, |H(o)| = \sigma_s^2 \, |H(o)|$$

(C.35)

The mean square value of the output is

$$\overline{V_{out}^2} = E\{V_{out}^2\} = R_{out}^{s+n}(o)$$

$$= \sigma_s^4 \ |H(o)|^2 + \int_{-\infty}^{\infty} \frac{2\sigma_n^4}{B_{HF}} \ |H(j\omega)|^2 \ df$$

$$+ \int_{-\infty}^{\infty} \frac{4\sigma_s^2\sigma_n^2}{B_{HF}} \ |H(j\omega)|^2 \ df \tag{C.36}$$

The output variance is

$$\sigma_{out}^2 = E\{V_{out}^2\} - E^2\{V_{out}\} = \int_{-\infty}^{\infty} \frac{2\sigma_n^4}{B_{HF}} \ |H(j\omega)|^2 \ df$$

$$+ \int_{-\infty}^{\infty} \frac{4\sigma_n^2\sigma_s^2}{B_{HF}} \ |H(j\omega)|^2 \ df \tag{C.37}$$

The relative deviation of the output is given by (Tiuri, 1964)

$$\sigma_{out}^* = \frac{\sigma_{out}}{E\{V_{out}\}} =$$

$$= \frac{\left[ \int_{-\infty}^{\infty} \frac{2\sigma_n^4}{B_{HF}} \ |H(j\omega)|^2 df + \int_{-\infty}^{\infty} \frac{4\sigma_s^2\sigma_n^2}{B_{HF}} \ |H(j\omega)|^2 \ df \right]^{1/2}}{\sigma_s^2 \ |H(o)|}$$

$$= \left[ 2 \left( \frac{\sigma_n^2}{\sigma_s^2} \right)^2 \frac{B_{LF}}{B_{HF}} + 4 \left( \frac{\sigma_n^2}{\sigma_s^2} \right) \frac{B_{LF}}{B_{HF}} \right]^{1/2} \tag{C.38}$$

where

$$B_{LF} \equiv \int_{-\infty}^{\infty} \left| \frac{H(j\omega)}{H(o)} \right|^2 df$$

(C.39)

The sensitivity of a radiometer is defined as the input signal which will give a D. C. output voltage equal to or greater than the effective value of the output fluctuations due to system noise (Tiuri, 1964). Thus if we consider an output signal to noise voltage ratio $\alpha$ (a figure of merit for the receiver), the equation governing the sensitivity of a receiver is

$$\frac{1}{\alpha} = \frac{\sigma_{out}}{E \{ V_{out} \}}$$

(C.40)

or from equation (38)

$$2 \left( \frac{\sigma_n^2}{\sigma_s^2} \right)^2 \frac{B_{LF}}{B_{HF}} + 4 \left( \frac{\sigma_n^2}{\sigma_s^2} \right) \frac{B_{LF}}{B_{HF}} = \frac{1}{\alpha^2}$$

(C.41)

For a perfect integrator (see Appendix B), the low frequency bandwidth can be written

$$B_{LF} = \frac{1}{2 \tau_I}$$

(C.42)

Using this relation, equation (41) can be written as

$$\left( \frac{\sigma_n^2}{\sigma_s^2} \right)^2 \frac{1}{B_{HF} \tau_I} + 2 \left( \frac{\sigma_n^2}{\sigma_s^2} \right) \frac{1}{B_{HF} \tau_I} - \frac{1}{\alpha^2} = 0$$

(C.43).

This equation has the solution

$$\frac{\sigma_n^2}{\sigma_s^2} = \sqrt{\frac{B_{HF}\,\tau_I}{\alpha^2} + 1} - 1 \tag{C.44}$$

or

$$\sigma_s^2 = \frac{\sigma_n^2}{\sqrt{\frac{B_{HF}\,\tau_I}{\alpha^2} + 1} - 1} \tag{C.45}$$

where

$$\sigma_s^2 = \frac{A^2\,|A(j\omega_o)|^2}{2}$$

and using equation (32)

$$\sigma_n^2 = \frac{kT_{SN}}{2} \int_{-\infty}^{\infty} |A(j\omega)|^2\,df = \frac{kT_{SN}\,B_{HF}}{2}\,|A(j\omega_o)|^2 \tag{C.46}$$

Thus the sensitivity equation becomes

$$A^2 = \frac{kT_{SN}\,B_{HF}}{\sqrt{\frac{B_{HF}\,\tau_I}{\alpha^2} + 1} - 1} \tag{C.47}$$

where $A^2$ now represents the smallest power that can be detected for a given output signal to noise ratio.

Then since

$$\Delta P_{min} = A^2$$

<div align="right">(C.48)</div>

is the smallest power that can be detected at the receiver input, the equation of sensitivity for the active source is

$$\Delta P_{min} = \frac{T_{SN} \, k \, B_{HF}}{\sqrt{\dfrac{B_{HF} \, \tau_I}{\alpha^2} + 1} - 1}$$

<div align="right">(C.49)</div>

For a Dicke receiver, the sensitivity will be decreased by a factor of 1/2 (see Appendix B), thus

$$\Delta P_{min} = \frac{2 \, T_{SN} \, k \, B_{HF}}{\sqrt{\dfrac{B_{HF} \, \tau_I}{\alpha^2} + 1} - 1}$$

<div align="right">(C.50)</div>

In general this will reduce to

$$\Delta P_{min} = \frac{2 T_{SN} \, \alpha \, k \, B_{HF}}{\sqrt{B_{HF} \, \tau_I}} = 2 \alpha k T_{SN} \sqrt{\frac{B_{HF}}{\tau_I}}$$

<div align="right">(C.51)</div>

## POWER SATURATION OF MOLECULAR STATES

The expression for an absorption coefficient which is broadened by saturation is (Carter and Smith, 1948)

$$K_a(\nu) = \frac{K_a(\nu_o)}{\left(\dfrac{\nu - \nu_o}{\Delta\nu_o}\right)^2 + 1 + \dfrac{AP}{(\Delta\nu_o)^2}} \tag{D.1}$$

The expression for saturated line half width (at half intensity) is (Carter and Smith, 1948)

$$\Delta\nu = \Delta\nu_o \left(1 + \frac{AP}{(\Delta\nu_o)^2}\right)^{1/2} \tag{D.2}$$

where

$$K_a(\nu_o) = \frac{8\pi^2 \nu_o^2 n_o}{3 C k T \Delta\nu_o} |\mu_{jk}|^2 \quad cm^{-1}$$

$\Delta\nu_o$ = the unsaturated half line width

$P$ = the power density in $\dfrac{ergs}{cm^2 \, sec}$

$A = \dfrac{8\pi |\mu_{ij}|^2}{3 c h^2}$ the Einstein coefficient for induced emission.

The expression for the dipole moment of the 22.235 GHz water vapor transition is (King et al., 1947)

$$|\mu_{ij}|^2 = 0.165 |\mu_o|^2 \qquad \text{(D.3)}$$

where

$$|\mu_o| = 1.85 \times 10^{-18} \quad \text{e.s.u.}$$

thus

$$|\mu_{ij}|^2 = 5.65 \times 10^{-37} \quad (\text{e.s.u.})^2$$

The Einstein coefficient for induced emission then becomes

$$A = 3.59 \times 10^6 \quad \frac{cm^2}{erg - sec}$$

From equation (D.2) saturation effects will be negligible when

$$AP \ll (\Delta \nu_o)^2$$

Thus the arbitrary criterion will be

$$AP \leq (\Delta \nu_o)^2 \times 10^{-3}$$

From the information in Table 1 the following table of maximum power densities is obtained

| $\underline{h}$ | $\underline{(\Delta\nu_o)^2}$ | $\underline{P_{max}}$ |
|---|---|---|
| 30 km | $16.0 \times 10^{14}$ $Hz^2$ | $4.5 \times 10^2$ $\frac{watts}{m^2}$ |
| 50 km | $7.3 \times 10^{12}$ $Hz^2$ | $2.0 \times 10^0$ $\frac{watts}{m^2}$ |
| 70 km | $5.3 \times 10^{10}$ $Hz^2$ | $1.5 \times 10^{-2}$ $\frac{watts}{m^2}$ |
| 90 km | $6.8 \times 10^8$ $Hz^2$ | $1.9 \times 10^{-4}$ $\frac{watts}{m^2}$ |

The cross sectional area illuminated by an antenna of area $10 \ m^2$ at a distance of 1000 km (the minimum distance between source and receiver in an occultation experiment) is $1.9 \times 10^7 \ m^2$. Thus the power of the source can be on the order of 3 Kw before saturation must be considered at 90 km. At lower altitudes the source power can be much greater.

# REFERENCES

Barrett, A. H., The detection of the OH and other molecular lines in the radio spectrum of the interstellar medium, IEEE Transactions on Antennas and Propagation, AP-12, 822-831, 1964.

Barrett, A. H., J. W. Kuiper and W. B. Lenoir, Observations of microwave emission by molecular oxygen in the terrestrial atmosphere, Journal of Geophysical Research, 71, 4723-4734, 1966.

Buhl, D. and L. E. Snyder, Microwave receivers for molecular line radio astronomy, Nature Physical Science, 232, 161, 1971.

Burdic, W. S., Radar signal analysis, Prentice Hall, Inc., New Jersey, 1968.

Carlson, A. B., Communication systems, McGraw-Hill Book Company, New York, 1968.

Carter, R. L. and W. V. Smith, Saturation effect in microwave absorption of ammonia, Physical Review, 73, 1053-1058, 1948.

Chang, S. Y. and J. D. Lester, Performance characteristics of a 300 GHz radiometer and some atmospheric attenuation measurements, IEEE Transactions on Antennas and Propagation, AP-16, 588-591, 1968.

Clark, T. A. B. Donn, W. M. Jackson, W. T. Sullivan and N. Vandenberg, Search for microwave $H_2O$ emission in comet bennett, Astronomical Journal, 76, 614, 1971.

Cohn, M., F. L. Wentworth and J. C. Wiltse, High sensitivity 100 to 300 GHz radiometers, Proceedings of the IEEE, 51, 1227-1232, 1963.

Croom, D. L., Stratospheric thermal emission and absorption near the 183.31 GHz (1.64 mm) rotational line of water vapor, Journal of Atmospheric and Terrestrial Physics, 27, 235-243, 1965.

Croom, D. L., Stratospheric thermal emission and absorption near the 22.235 GHz (1.35 cm) rotational line of water vapor, Journal of Atmosphere and Terrestrial Physics, 27, 217-233, 1965.

Dicke, R. H., The measurement of thermal radiation at microwave frequencies, Rev. Sci. Instru., 17, 268-275, 1946.

Goldstein, S. J., A comparison of two radiometer circuits, Proceedings of the IRE, 43, 1663-1666, 1955.

Karplus, R. and J. Schwinger, A note on saturation in microwave spectroscopy, Physical Review, 73, 1020-1026, 1948.

King, G. W., R. M. Hainer and P. C. Cross, Expected microwave absorption coefficients of water and related molecules, Physical Review, 71, 433-443, 1947.

Klipper, H., Sensitivity of crystal video receivers with RF preamplification, Microwave Journal, 8, 85-92, August 1965.

Kraus, J. D., Radio astronomy, McGraw-Hill Publishing Company, New York, 1966.

Linsky, J. L., A recalibration of the quiet sun millimeter spectrum based on the moon as an absolute radiometric standard, Solar Physics, 28, 409-418.

Longbothum, R. L., Properties of water vapor relevant to its measurement in the stratosphere and mesosphere, Ionosphere Research Scientific Report No. 420, 1974.

Meredith, R. and F. Warner, Superheterodyne radiometers for use at 70 GHz and 140 GHz, IEEE Transactions on Microwave Theory and Techniques, MTT-11, 397-411, 1963.

Moody, H. J., Millimeter wave radiometry, Canadian Aeronautics and Space Journal, M-22 - M-26, 1971.

Rishbeth, H. and O. K. Garriott, Introduction to ionospheric physics, Academic Press, New York, 1969.

Staelin, D. H., Passive remote sensing at microwave wavelengths, Proceedings of the IEEE, 57, 427-439, 1969.

Staelin, D. H. Quarterly Progress Report No. 108, Research Laboratory of Electronics, M.I.T., 61, 1973.

Thomas, J. B., An introduction to statistical communication theory, John Wiley and Sons, Inc., New York, 1969.

Tiuri, M. E., Radio astronomy receivers, IEEE Transactions on Antennas and Propagation, AP-12, 930-938, 1964.

Waters, J. W., Private Communication, 1974.